Future Generation Computer Systems 155 (2024) 146–163

Contents lists available at ScienceDirect

Future Generation Computer Systems

journal homepage: www.elsevier.com/locate/fgcs

A digital twin-based energy-efficient wireless multimedia sensor network for waterbirds monitoring

Aya Sakhri [a,b], Arsalan Ahmed [a], Moufida Maimour [a,*], Mehdi Kherbache [a], Eric Rondeau [a], Noureddine Doghmane [b]

[a] CRAN Laboratory, Université de Lorraine, CNRS, UMR 7039, Campus Sciences, BP 70239, F-54000 Nancy, France
[b] LASA Laboratory, University of Badji Mokhtar, Annaba, Algeria

ARTICLE INFO

Keywords:
Waterbirds monitoring
WMSN
Audio classification
Energy efficiency
Digital twin
Dynamic control

ABSTRACT

Wetlands play a critical role in maintaining the global climate, regulating the hydrological cycle, and protecting human health. However, they are rapidly disappearing due to human activities. Waterbirds are valuable bio-indicators of wetland health, but it is challenging to monitor them effectively. Wireless Multimedia Sensor Networks (WMSNs) offer a promising technology for monitoring wetlands. Nonetheless, these networks are constrained in terms of energy, and also encounter challenges associated with large-scale deployments under natural environmental conditions. These conditions introduce harsh circumstances that may not have been anticipated during the pre-deployment testing phase. This paper proposes a Digital Twin (DT) based energy-efficient WMSN monitoring system specifically tailored for waterbirds in wetlands. The system utilizes a unique approach that combines local audio identification and image compression with DT technology to optimize network performance and minimize energy consumption. To reduce unnecessary image transmissions, the system employs a real-time, low-complexity local audio identification phase before triggering image capture. A denoising step is employed to achieve highly accurate bird recognition despite surrounding noises. Each image undergoes a low-complexity compression scheme prior to transmission, further enhancing energy efficiency. To enhance the system's overall efficiency and effectiveness, DT technology is integrated to create real-time replicas of the WMSN and the monitoring application. A synergistic interaction between the two DTs enables cooperative data-making decision that ensures both QoS (Quality of Service) and QoE (Quality of Experience) requirements are met. Transmission rate control is done using a fuzzy logic decision-making technique. Real-time feedback provides rapid and accurate analysis of the current state of the WMSN, allowing for dynamic adjustments. The "what-if scenarios" feature of the implemented DTs has been effectively leveraged to find the most suitable settings for the controller. The effectiveness and performance enhancements achieved by integrating DT into our WMSN-based surveillance system are validated through comprehensive experiments in scenarios that correspond to a real-world wetland. Comparative analyses demonstrate the undeniable benefits of the DT-integrated system compared to a conventional WMSN-based surveillance setup. In particular, the results demonstrate the system's superior performance in terms of energy efficiency, real-time monitoring capabilities, and ability to handle multiple video sources.

1. Introduction

Wetlands are universally recognized as one of the most valuable and precious resources for this planet, serving a critical role in the preservation of biodiversity, maintenance of the global climate, regulation of the global hydrological cycle and protection of human health [1]. Due to their immense importance, wetlands are extremely vital for the well being of human societies and should be conserved at all costs. Unfortunately, of late, there has been a rapid global decline in both the area as well as quality of wetlands. Approximately, 64% to 71% of the world's wetlands were lost in the previous century [2]. More recently, it is estimated that their rate of disappearance is three times faster as compared to that of forests [3]. This translates into a major

* Corresponding author.
E-mail addresses: aya.sakhri@univ-lorraine.fr (A. Sakhri), arsalan.ahmed3@etu.univ-lorraine.fr (A. Ahmed), moufida.maimour@univ-lorraine.fr (M. Maimour), mehdi.kherbache@univ-lorraine.fr (M. Kherbache), eric.rondeau@univ-lorraine.fr (E. Rondeau), ndoghmane@univ-annaba.org (N. Doghmane).

https://doi.org/10.1016/j.future.2024.02.011
Received 25 August 2023; Received in revised form 25 December 2023; Accepted 12 February 2024
Available online 13 February 2024

deprivation of the ecosystem services that wetlands provide, resulting in a potential annual loss of up to $20 trillion [2]. This degradation and loss of wetlands could largely be attributed to the harmful modern trends of climate change, overpopulation, rapid urbanization, pollution, agricultural intensification and over-utilization of resources.

Given this context, it is necessary to routinely observe, track and monitor the state of wetlands. The purpose of monitoring is to extract useful insights for performing ecological assessment of the target ecosystem. However, it is not possible and practical to monitor all components of the ecosystem and therefore, few of them should be selected as indicators of the overall environmental conditions. Several researchers have demonstrated that waterbirds are valuable bio-indicators for assessing the status of wetlands as they exhibit responsive behaviors to changes in their environment [4,5]. Therefore, usage of waterbirds as indicators of wetland health is justified especially when 38% of all the existing waterbirds species are on the decline [6].

In order to monitor and assess waterbirds' population in wetlands, WMSNs could be deployed [7]. Unlike typical Wireless Sensor Networks (WSNs), WMSNs are equipped with multimedia devices that are capable of retrieving acoustic and visual information in addition to the scalar sensor data. WMSNs are a good choice for waterbirds monitoring since a specific waterbird species could be easily identified based on its vocalization and/or photographs. Furthermore, WMSNs are well-suited for operating under the harsh and challenging conditions presented by wetlands. However, WMSNs have inherent limitations in terms of energy, memory, and bandwidth, which pose significant challenges. Specifically, the energy aspect holds prime importance, particularly due to the deployment of hundreds of nodes in natural environments like wetlands, causing difficulties with battery replacement. Consequently, one of the goals is to ensure efficient network utilization by extending the lifetime of the nodes as much as possible. Notably, image processing and transmission are the major energy-consuming stages in a WMSN-based surveillance system. Therefore, it is essential to minimize the volume of the captured and transmitted visual data. In addition, the large-scale deployments of WMSNs are quite challenging under natural environmental conditions. This is because natural surroundings present harsh circumstances, previously unseen during the pre-deployment testing stage, which could cause bugs and performance degradation in the deployed WMSN. The negative influences from the numerous constraints and unknowns could not be extensively modeled only with the help of simulations and testbeds inside laboratories [8].

Addressing these issues, this paper proposes an energy-efficient WMSN monitoring system specifically tailored for waterbirds in wetlands. The system leverages local audio preprocessing for intelligent identification, effectively reducing unnecessary image transmissions and optimizing resource utilization. Additionally, digital twin (DT) technology is integrated to create real-time replicas of the WMSN and the monitoring application, enabling cooperative dynamic control for optimal performance. Key contributions of this work include :

- A low-cost audio preprocessing is employed to identify birds despite surrounding noises, thanks to a prior denoising step. This reduces unnecessary image transmissions. Each image undergoes a low-complexity compression scheme prior to transmission, further enhancing energy efficiency ;
- Our DT implementation features a real-time feedback mechanism, enabling rapid and accurate analysis of the current state of the WMSN. This drives dynamic fuzzy logic control of the data rate ensuring a balanced approach between efficient resource utilization and surveillance quality ;
- What-if scenarios has been effectively leveraged to find the most suitable settings of the controller, including fuzzy set definition and control rules, as well as the control periodicity. The results demonstrated good responsiveness while maintaining system stability ;
- The collaboration between the network and application DTs empowers the system's efficiency by intelligently controlling the transmission rate to meet both QoS and QoE demands ;
- The effectiveness and performance enhancements achieved by integrating DT into the WMSN-based surveillance system are validated through comprehensive experiments in scenarios that correspond to a real-world wetland.

The remainder of this paper is organized as follows. Section 2 provides an introduction to DT paradigm and fuzzy logic control principles laying the foundation for understanding the proposed system. Section 3 delves into the related work on waterbirds monitoring and the utilization of DT technology for natural environment surveillance. The proposed system is described in Section 4. Section 5 elaborates on the experimental details along with the specific research use-case considered for the DT-based control. The experimental results are discussed in Section 6. Finally, Section 7 concludes the paper.

2. Background

2.1. Digital twin technology: An overview

The evolution of the DT concept began in 2002, when Prof. Grieves introduced it in the Product Lifecycle Management (PLM) course at the University of Michigan [9]. After a period of a slow development from 2003 to 2011 [10], technological advancements in sensor technology, IoT, big data analytics, simulation technologies, machine learning (ML), and computational infrastructure propelled the rise of DT technology. NASA's formalization of the DT concept and its potential to enhance performance in aetronautics and aerospace further boosted its popularity [11]. In 2014, Grieves expanded its scope from a conceptual idea to numerous practical applications [12]. Since then, DT applications have gained significant traction, becoming one of the top-ten most promising technology trends for the upcoming decade [13]. Despite the burgeoning interest in DTs, a common thread among various interpretations, is the notion of a DT as a virtual mirror, providing an all-encompassing reflection of the attributes of the real physical system. Key to DTs is the seamless synchronization between the physical and virtual realms. Unlike mere simulations, DTs can access real-time data from their physical counterparts, ensuring continuous and dynamic updates. This continuous update mechanism enables DTs to serve as powerful tools for optimizing performance, predicting failures, and improving decision-making across a wide range of applications.

A DT is composed of four fundamental components [14]. The physical part embodies the tangible asset, system, process, or environment that corresponds to the physical twin. It is the real-world counterpart that is being mirrored in the virtual world. The digital part is the core essence of the DT concept. It is the virtual counterpart of the physical element. This digital representation serves as a source of valuable insights, enhancing the comprehension of the physical entity. It can be used to visualize the physical system, simulate its behavior, and predict its future state. The data feed plays a pivotal role in supplying the DT with real-time information regarding its physical counterpart. The specifics of data collection are tailored to the unique requirements of the particular application use case. Data feeds can come from a variety of sources, including sensors, databases, and external systems. Interventions are the actions that are taken based on the insights gained from the digital part. They can be used to optimize the performance of the physical twin, prevent failures, and improve decision-making.

A common misconception in DT research involves the level of integration within DT systems, which is determined by the extent of information exchange between the physical and digital counterparts [15]. This distinction separates genuine DTs from digital models and shadows. In digital models, there is no automatic data synchronization between the physical and digital parts. Digital shadows exhibit a one-way automatic synchronization from the physical entity to its digital counterpart. The digital representation is continuously updated with real-time data, but the feedback loop is unidirectional. Digital Twins, on the other hand, embody the highest level of integration, boasting two-way automatic data synchronization between the physical and digital components. This bi-directional exchange enables real-time data flow, allowing for the digital representation to not only reflect the physical system's state but also influence it through simulated interventions. Unfortunately, many DT researchers fail to explicitly classify their implementations by integration level, leading to the broader application of the term "DT" to encompass digital models and shadows.

2.2. Decision-making based on fuzzy logic

Fuzzy logic, introduced by Zadeh in 1965 [16], is a mathematical framework designed to address the intricacies of imprecision and uncertainty in decision-making [17]. Its core concept is the notion of *fuzzy sets*, which depart from traditional binary sets where elements either unequivocally belong (with a degree of 1) or do not belong (with a degree of 0). Instead, fuzzy sets allow elements to belong to a certain degree, represented by a value between 0 and 1, capturing the essence of partial membership. *Membership functions* serve to quantify this level of belonging, employing various shapes like triangular, trapezoidal, or Gaussian to represent diverse levels of uncertainty.

Fuzzy logic commonly operates on linguistic variables, which represent concepts using linguistic terms like *"Bad"*, *"Good"*, and *"Ideal"*. Each linguistic term is assigned a fuzzy set with associated membership functions that define its range of applicability. Fuzzy rules, expressed in the form of *"IF-THEN"* statements, establish relationships between input variables and output variables. They embody linguistic reasoning capabilities, allowing systems to make decisions based on imprecise or qualitative information.

The fuzzy inference system orchestrates the fuzzy rules to determine the degree of satisfaction of each rule in light of the current input values. It employs logical operators like *"AND"*, *"OR"*, and *"NOT"* to combine the fulfillment degrees of individual conditions within each rule. Following the evaluation of fuzzy rules, the next step involves aggregating the results from multiple rules to obtain a crisp, non-fuzzy output value. This process, known as *defuzzification*, translates the fuzzy logic reasoning into a single, definitive decision.

3. Related work

3.1. Energy-efficient WMSN-based monitoring strategies

In a WMSN, image processing and transmission are the two most energy-consuming stages. In order to reduce the size of visual data that needs to be processed and transmitted, several strategies have been proposed in the literature. One such strategy is to use low-complexity and energy-efficient image compression algorithms adapted for WMSNs [18,19]. Other various research endeavors [20–22] have been carried out with the objective of detecting and extracting objects in images. The underlying principle of this approach is the extraction of salient information and subsequent transmission of significantly reduced data in comparison to the original visual data. Only the portions of the images that encompass a mobile object are communicated via the network, instead of the entire video. In a related study [23], a novel probabilistic approach for WMSNs is proposed leveraging object presence detection and an image transmission scheme. Specifically, when an object is detected in the scene, only the relevant area containing the object is transmitted using 2D-DWT coding. The authors assert that their approach significantly reduces node energy consumption, achieving an impressive 95% energy savings. In [24], the authors introduce an efficient technique for object classification that operates locally on a camera sensor. This method employs two object features of the video images : the minimum object bounding box shape and the object velocity in the monitored area. The authors assert that satisfactory classification accuracy can be achieved without imposing substantial demands on the storage and energy resources of the camera sensors. Other approaches to reduce the amount of multimedia data at the sensor node involves using recognition schemes. For instance, in [25], the authors present an energy-efficient scheme for moving target detection using a two-tiered cluster-based WMSN, which they claim reduces network energy by 65% compared to other methods in the literature. Moreover, [26] presents an innovative method for image-based object identification in WMSNs using object shape features. Their work focuses on the development of a low-complexity scheme that utilizes image processing techniques to identify target objects. The authors contend that their approach performs exceptionally well in identifying specific targets while imposing minimal power processing requirements when compared to image transmission.

An alternative strategy for reducing the volume of visual data transmitted involves online video summarizing, as proposed in [27]. This technique involves a low complexity algorithm that eliminates redundant frames from the captured video stream. Initially, each input frame is represented by extracting representative features, which are then clustered using an online Gaussian mixture model. The decision to retain or discard a frame is based on the clustering outcomes. Background subtraction represents another technique for extracting foreground objects in videos, as discussed in several studies such as [28–30]. For instance, [29] proposes an efficient compression-based background subtraction approach aimed at minimizing object extraction and transmission energy in WMSNs. This method employs compression on the difference frame. A foreground threshold is subsequently applied to the resulting difference measurements to determine those that will be utilized to reconstruct the foreground. As a result, only the pertinent measurements are transmitted instead of the entire video. In addition, several investigations, such as the work conducted by [31], have employed motion detection as a mechanism for energy-efficient image transmission. Specifically, the camera is activated solely upon the detection of motion by the corresponding sensors in the surrounding vicinity. We mention [32], where the authors propose an architecture of sensor nodes equipped with a camera and a Passive Infrared Sensors (PIR). The video processing module is only triggered when a moving object is detected by the PIR sensor.

Despite the reduction in the size of transmitted video data resulting from the above-mentioned techniques, the processing or/and transmission of unnecessary images can proceed when non-interest images are captured, leading to excessive energy consumption. To the best of our knowledge, there have been only a limited number of studies that attempt to integrate audio and visual data in sensor networks to achieve energy-efficient operations. In this context, we highlight [33], where they propose an energy-efficient architecture for combining visual and audio data in a sensor node to detect and recognize various threats and objects. However, their model is not designed to address complex environmental noise conditions, which poses a significant constraint in our application. Therefore, improving the local audio design constitutes a primary necessity.

3.2. Digital twin for monitoring natural environments — application and network perspective

Over the span of the last two decades, the notion of DT has evolved from a mere idea to a well-established concept. In simple terms, a DT is defined as an accurate virtual model designed to reflect the state of a physical entity for the purpose of optimization [34]. More recently, DTs are being increasingly developed not only for the traditional engineering applications but also for various aspects of natural environments. Specifically, the integration of DTs with the monitoring systems dedicated to natural environments, such as wetlands, enables a more comprehensive understanding and improved management of these ecosystems [35]. Such DTs could well become the game changers for researchers and environmentalists in their efforts to preserve the natural world amidst the global environmental crisis.

In the context of WMSN-based monitoring systems, the associated DT could be developed from two perspectives : application perspective and network perspective. Application DT (ADT) refers to the virtual

Table 1
Summary of related work : using DTs in natural environment surveillance.

Ref.	Target environment	Implementation	Networking considerations	Main contribution
[36]	Mountain	Theoretical framework	✓	A DT architecture for early warnings of geological disasters in mountainous regions is proposed with discussion of implementation methods.
[37]	River-basin	Methodological guidance	✓	Discussion on the key technologies required to realize DTs of riverbasins and proposal of a technical framework.
[38]	Forest	Reference framework	✓	Proposal of a framework to design a forest DT for the enhancement of sustainable forest management practices.
[39]	Mountain	Theoretical framework	✓	Discussion on adopting digitally enhanced disaster risk reduction strategies through Territorial DTs to promote evidence-based decision-making and community engagement.
[40]	River	High level architecture	✗	Laying of the foundation for an Earth system DT for flood prediction and analysis along with a high level architecture.
[41]	Forest	Theoretical analysis	✗	A DT architecture for virtual plantation forest modeling and data analysis is proposed to enhance forestry research and management.
[42]	Wetland	Prototype	✓	A DT architecture for early warning of geological disasters in mountainous regions with discussion of implementation methods.
[43]	Flood	Prototype	✓	Presentation of *StormSense*, a DT platform for flood management and coastal resilience planning.
[44]	Dam & watershed	Prototype	✓	Development of a DT platform for dam and watershed management, using real-time data and simulation models for flood response and water resource management.
[45]	Air	Prototype	✗	Presentation of a DT for a complex airfield ecosystem, represented as a geometrically configured point cloud, to assess air quality in the controlled area of an airport.
[46]	Ocean	Prototype	✓	Use of DTs for monitoring, operation and maintenance of an underwater network of ocean observation systems.
[47]	River	Prototype	✓	Using timely and accurate satellite data to calibrate a 2D hydraulic model for simulating a levee breach event.
Ours	Wetland	Prototype	✓	A novel WMSN system that utilizes local audio processing to recognize waterbirds. Application and network DTs cooperation is featured for optimal performance.

representation of the high-level application running on the sensor network, such as waterbirds monitoring, that captures the behavior and functionalities of that specific application. On the other hand, the network DT (NDT) is the digital representation of the physical network itself. Hence, the ADT predominantly prioritizes the QoE by replicating the application-level behavior. In contrast, the NDT places greater emphasis on QoS, focusing on the performance and reliability of the network infrastructure.

While there has been some recent research on the application of DTs for monitoring natural environments, many of these studies fail to fully embrace the true potential of DTs by implementing only one-way or manual data synchronization mechanisms. For instance, [48] proposes a DT system for understanding the relationship between urban expansion and the nearby natural environment, but it does not implement an automatic two-way data synchronization mechanism. Similarly, other studies, such as [49–51], also fall short of implementing a true DT by relying on digital models. On the other hand, studies such as [52–56] concern digital shadows where only one-way automatic synchronization exists from the physical part to its digital replica. For instance, [56] presents a DT system prototype for the purpose of increasing meaningful engagement of children with the natural world.

Table 1 summarizes existing research efforts in the domain of digital twins for natural environment monitoring, focusing on those concerned with true digital twins, where there is automatic control feedback and real-time updates to the model based on real-world data. While the literature primarily discusses the ideas, frameworks, and technologies for developing digital twins in various natural environments, there are limited real-world implementations. For instance, [42] proposes a reference architecture for digital twins in wetlands, incorporating mass personalization capabilities, while [46] utilizes digital twins for monitoring, operation, and maintenance of underwater ocean observation systems.

While developing DT-based solutions for natural environments, a common tendency is to focus primarily on the creation of the DT model for the target environment, often assuming that the underlying monitoring infrastructure will be readily deployed without any challenges. However, this assumption often falls short in complex natural environments, particularly in large-scale deployments. Unfortunately, many researchers overlook or underestimate the crucial role played by networking and communication aspects, which are fundamental pillars of the DT concept. Despite the inclusion of networking considerations in some studies [36–39,42–44,46,47], these aspects often receive superficial treatment, lacking detailed technical specifications and chiefly focusing on logical architectures. Thoroughly integrating networking considerations when developing DTs is essential for ensuring their seamless operation and maximizing their potential. This goal can be effectively achieved by considering the creation of a DT for the network itself, providing a more comprehensive approach that encompasses both network and application requirements.

Numerous research efforts have delved into the concept of the network DT (NDT), exploring a range of architectures, modeling perspectives, and techniques, alongside proposing a variety of networking services. These endeavors aim to fully unlock the transformative potential of the DT paradigm within the networking domain [57]. IETF is actively spearheading the standardization of the NDT concept. Their latest draft [58] provides an insightful overview of the core concepts, a reference architecture, and the primary challenges associated with building an NDT. [59] introduces a machine learning-driven NDT as an indispensable tool for effectively controlling and managing modern networks. Another study [60] presents a holistic architecture for NDT in wireless systems. Addressing the complexities of NDT modeling and data collection, [61] proposes a four-layer architecture. [62] showcases an NDT leveraging graph neural networks to predict global QoS and model intricate network characteristics.

The existing literature underscores significant advancements in the development of ADTs for natural environment monitoring applications, as well as general NDTs. While some studies have incorporated networking aspects, the maximum potential for WMSN-based monitoring systems lies in the collaborative integration of these two

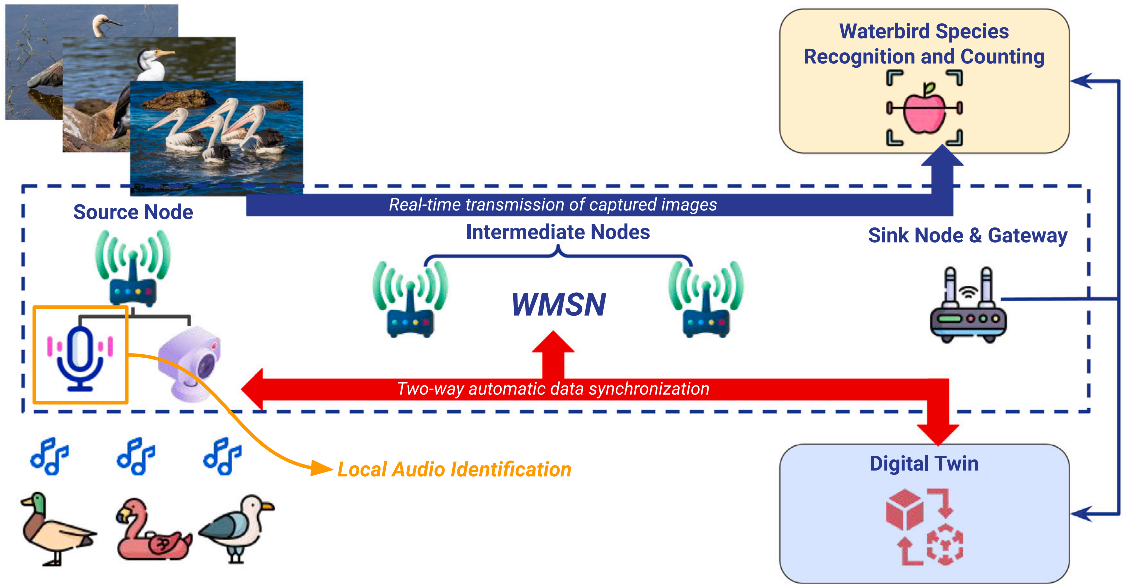

Fig. 1. Integration of DT technology with the energy-efficient WMSN encompassing local audio classification.

approaches. To the best of our knowledge, no previous studies have explored the combined utilization of application and network DTs to enhance the performance of WMSN-based monitoring systems, particularly for natural environment-related applications such as waterbirds monitoring. Therefore, our research is centered on this dual-perspective collaboration.

4. Digital twin-based WMSN efficient monitoring

The primary objective of our surveillance system is to accurately identify, recognize and count the population of specific waterbird species. To do so, we propose a WMSN monitoring infrastructure (Fig. 1) that incorporates source nodes equipped with audio and image sensors to capture their vocalizations and photographs. These source nodes are assumed to be independent of each other, capturing audio and images that effectively lie outside each other's field of view. The network consists of multiple intermediate nodes that facilitate packet forwarding towards a collect station (the sink). To prolong the network lifespan by reducing the energy consumed per node for visual data processing and transmission, we suggest implementing a preliminary local audio identification phase (Section 4.1) prior to activating the camera. Rather than capturing and transmitting to the sink at all times, the image sensors are activated based on the outcomes of an audio identification process. Prior to the transmission, the captured images undergo a low complexity compression and encoding technique (Section 4.2) to further save energy and resources.

The captured images need to be transmitted and delivered to the sink in real-time (*almost*) ensuring that the monitoring system is continuously updated with the most current information about the wetland environment. Furthermore, it is essential that the images delivered to the sink are of high quality to enable effective application of waterbirds species recognition and counting processes, which are the ultimate goals of the system. However, similar to any WMSN, this system is also prone to faults and issues that can impede the effectiveness of species recognition and counting procedures. For instance, network congestion can result in packet losses, which in turn may degrade the quality of images received at the sink. Hence, a DT implementation for this system is invaluable for continuously tracking the WMSN. This way, the DT can detect any anomalies in real-time and take adequate corrective measures to optimize the system's performance.

The integration of a DT with the WMSN is depicted in Fig. 1. The real-time image data captured by the source node, based on the local audio identification, traverses the network, passing through intermediate nodes, to reach the sink node. The sink node serves as a gateway, forwarding the data to an end system, which is hosted remotely, for the purpose of waterbirds recognition and counting. Concurrently, the DT is connected to the sink node and actively monitors the WMSN leveraging the bidirectional connectivity. This automatic two-way data synchronization not only enables the DT to have real-time knowledge of the system but also allows it to intervene when necessary. The interventions may involve making modifications either at the source node or within the traffic carrying network.

Although ADT and NDT have distinct focuses, collaboration between them allows for a comprehensive understanding and effective management of the associated system, considering both the end-user requirements as well as the underlying network characteristics. This dual perspective enables a holistic approach to system analysis, control and optimizations. Fig. 2 depicts this collaboration between the ADT and the NDT. Data gathered from the WMSN-based monitoring system is utilized to update both the ADT and the NDT. The up-to-date information on the QoE and QoS from the ADT and the NDT, respectively, is then used to assess the current state of the system. Subsequently, appropriate optimization measures are communicated to the real-system in order to enhance its performance. It is to be noted that all of these operations occur dynamically and in real-time while the system is actively running.

4.1. Local audio identification

We have previously described our real-time audio identification phase in [63,64]. During this phase, audio signals from the surrounding environment are regularly sampled. First, the captured audio signal undergoes a denoising process to remove any unwanted noise present in the signal. This denoising process is based on the geometric approach to spectral subtraction presented in [65]. Next, the Mel Frequency Cepstral Coefficients technique [66] is applied to the captured audio signal to extract the distinctive and representative features while eliminating non-useful information. Lastly, utilizing the Dynamic Time Warping (DTW) distance with a threshold-based matching approach [67], the extracted features are compared to the reference waterbird sounds. This comparison allows for the classification that whether the captured audio signal corresponds to the presence of a waterbird or not. Only when the processing of the captured audio signal detects the presence of a waterbird, the camera is activated to capture an image, which

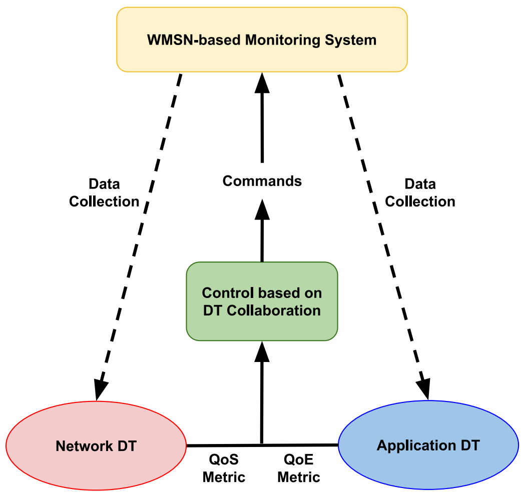

Fig. 2. Collaboration between the application DT and the network DT.

is subsequently transmitted to the sink node. Therefore, the audio identification serves as the determining factor for capturing the images.

4.2. Image encoding at the source

To reduce power consumption due to data transmission in our constrained WMSN, it is necessary to compress the visual data to a considerable extent before transmitting it to the end user. To address this requirement while saving energy and limiting processing resources, we use a low-complexity image compression method provided by SenseVid [68]. A captured image to be transmitted is broken down into 8×8 blocks. Subsequently, a low complexity DCT (binDCT-C) is applied on every block using a triangular pattern, taking into account solely the coefficients situated in the upper left triangle, with a side length $\rho = 8$. This reduces the complexity of the DCT and optimize its processing by eliminating redundant coefficients. The DCT block coefficients are quantified using the standard JPEG quantization matrix. The resulting block is then subject to traditional zigzag scanning. Finally, lossless entropy coding is employed using exponential-Golomb. Fig. 3 depicts the encoding steps.

In quantization, lossy compression is achieved by reducing the number of bits needed to store an integer value. This significantly reduces the size of an image enabling efficient storage and transmission along with energy savings. However, it is to be noted that quantization introduces a trade-off between compression rate and the resulting image quality. The higher is the compression rate, the lower is the image quality and vice versa. This trade-off could be achieved by adjusting the quantization matrix values through the selection of a proper quality coefficient (QC). A QC value of 1 corresponds to the poorest visual quality while a value of 100 results in the best possible quality.

4.3. Image quality evaluation at the sink

In our monitoring system, the sink node must assess the quality of the received images without any available reference (transmitted images). As a result, we suggest to use the Blind/Referenceless Image Spatial Quality Evaluator (BRISQUE) metric [69] to assess the quality of the received images. BRISQUE is a no-reference metric, specifically designed to quantify the distortion in a digital image without access to the original reference which is in close resemblance to how humans visually perceive images. It is a holistic metric that leverages scene statistics to accurately quantify potential losses of *naturalness* in an image caused by distortions. Its performance is statistically comparable to other full-reference metrics such as Peak Signal-to-Noise Ratio (PSNR) and the Structural Similarity Index Measure (SSIM) [70], while maintaining low computational complexity making it suitable for real-time applications. For an input image, BRISQUE provides a quality score between 0 and 100, where lower scores indicate better perceptual quality.

Our application and network digital twins have been harnessed to conduct what-if scenarios, offering a valuable tool for parameterizing our controller (Section 4.4), ensuring its ability to seamlessly adapt to diverse operating conditions and achieve optimal performance. Through the simulation of hypothetical scenarios, we can meticulously explore the controller's behavior under a wide range of input and output combinations, enabling us to fine-tune its parameters for enhanced performance. Specifically, what-if scenarios have been executed to evaluate the impact of varying quantization parameters (QCs) on the BRISQUE scores of compressed images. Three distinct wetland scenes are selected encompassing different waterbirds. Snapshots of each of these three scenes are shown in Fig. 4. Fig. 5(a) shows the relationship between the value of QC and the average BRISQUE score *(before transmission)* of the compressed images across the three scenes. For a given QC value, the BRISQUE scores across 30 consecutive images of a single scene are averaged out. It can be seen that with the rise in the value of QC, there is a corresponding decrease in the average BRISQUE score that plateaus around a value of 30. In our case, we are considering the desired or acceptable value of the BRISQUE score to be 38, as indicated by the dashed line in the graph. The selection of this value is guided by our internal researchers involved with the waterbirds monitoring application, where the images are intended for waterbird species recognition and counting purposes. It is to be noted that this value is subject to variation depending upon each individual application. The zoomed-in section of the graph highlights that each scene achieves the ideal BRISQUE score at a different QC value. Hence, the QC value at the source nodes cannot remain constant but needs to be adjusted depending on the specific image. Additionally, adopting consistently a high QC value may indeed achieve the desired BRISQUE score; however, it would negatively impact the transmission datarate and energy consumption at the source nodes. Figs. 5(b) and 5(c) demonstrates the relationship between the value of QC with the average datarate and the average encoding energy *(before transmission)*, respectively. It is clear from the figures that with the rise in the value of QC, both the average datarate as well as the average encoding energy continually increases. This reinforces the notion that excessively high QC values are detrimental for the system as it escalates the energy consumption while increasing the risk of network congestion. For this reason, selecting the right QC value (in this case, within the black vertical lines) is crucial in ensuring optimal system performance where the BRISQUE score is ideal, energy consumption is minimal and potential network congestion is mitigated.

So far, the discussion has been about the effect of QC on the compressed images at the source nodes. However, it is important to note that these images are to be transmitted through the network to reach the sink node. Packet losses on the network can result in a deterioration in the final BRISQUE score of the image upon reception. Therefore, the Packet Delivery Ratio (PDR) for a transmitted image is also significant alongside QC in determining the image quality at the sink node. Fig. 6 depicts the relationship of QC and PDR on the values of average BRISQUE score at the sink node for wetland scene 1 (Fig. 4(a)). As expected, for a value of QC, the average BRISQUE score decreases with the increase in PDR. This is logical as a higher PDR value corresponds to a lower number of missing components, resulting in better image quality.

4.4. DT-based decision making: Fuzzy logic based dynamic control

In order to validate the proposed integration of DT technology within the energy-efficient WMSN-based waterbirds monitoring system, a specific research use-case is considered, involving the compression

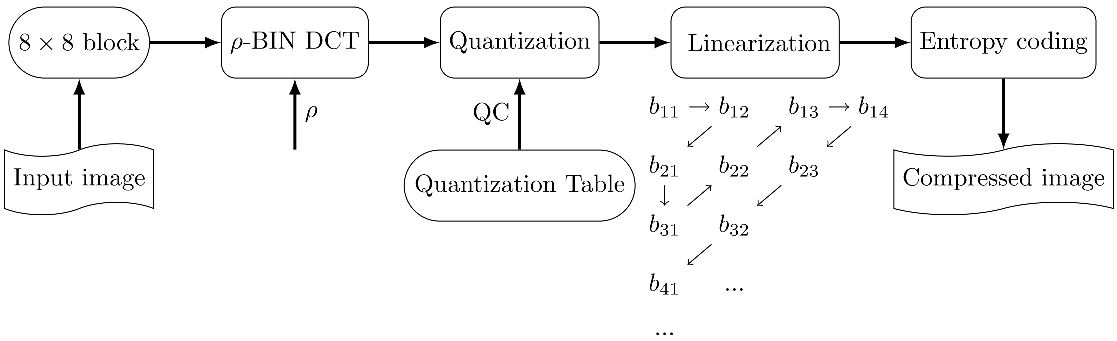

Fig. 3. The encoding sequence of M-frame block.

(a) Scene 1 (b) Scene 2 (c) Scene 3

Fig. 4. Snapshots of three different wetland scenes used for understanding the impact of QC.

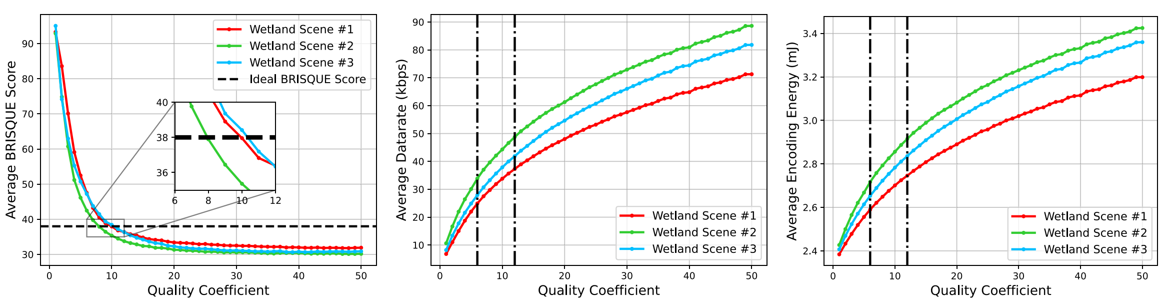

(a) Average BRISQUE Score (b) Average Datarate (c) Average Encoding Energy

Fig. 5. Effect of varying QC on the BRISQUE score, datarate and encoding energy of the compressed images *(before transmission)*.

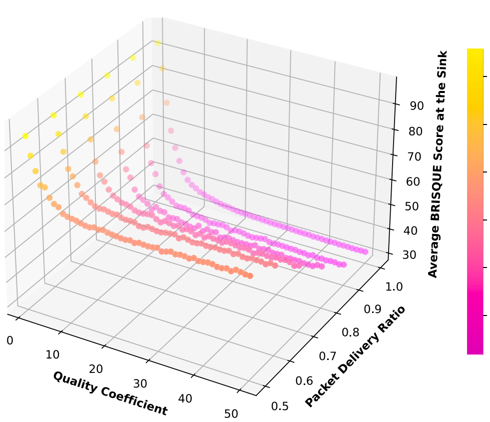

Fig. 6. 3D scatter plot of average BRISQUE score with varying QC and PDR *(after transmission)* at the sink for wetland scene 1.

rate of the captured images at the source nodes. We suggest to establish an algorithm that interacts with the ADT and the NDT to monitor the network as well as the quality of the received images at the sink node. Based on this, informed decisions are made regarding the adjustment in the compression rate (via the value of QC) at the source nodes. By leveraging the real-time information of the system available from the DT, performance could be optimized while the system is actively running. It is important to note that image quality is also influenced by parameters other than QC such as the triangle side length ρ introduced in Section 4.2. Fig. 3 depicts its incorporation into the encoding process. For additional parameters, the reader is referred to [68]. However, in this work, only QC is being studied because it has the most significant contribution to image quality. Moreover, considering the numerous components and complexity of the WMSN-based waterbirds monitoring system, it is impractical to develop an associated DT system that encompasses all its aspects at an early research stage. Therefore, in terms of the DT aspect, our focus is specifically on the transmission of captured waterbird images, without addressing the audio-related components of the system. Certainly, the initial audio identification process does play a role in reducing energy consumption at the source and improving overall network traffic, thereby enhancing system performance. However, the DT is not directly involved in the functioning of the audio component.

The fuzzy logic-based decision-making process utilizes two input variables and one output variable. Specifically, the up-to-date BRISQUE scores and PDR values of the last received image at the sink from each source node, serve as the input parameters. These inputs are then employed to calculate the appropriate change in the value of

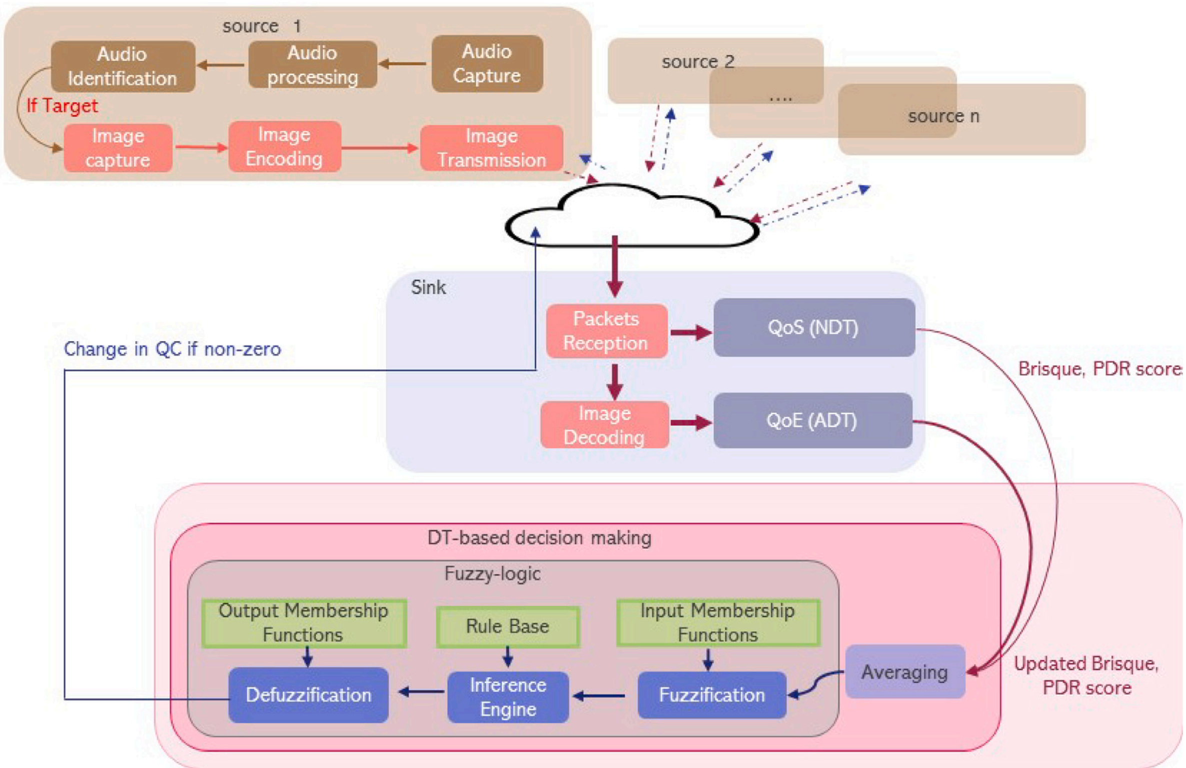

Fig. 7. Flow of the DT-based dynamic control approach.

QC that needs to be applied at the respective source node. Here, the distinction between BRISQUE as an application-related metric and PDR as a network-related metric is evident. Therefore, we utilize this dual perspective of the application as well as the underlying network to enhance the performance of the WMSN. The sink computes the features and performs real-time updates to both the ADT and the NDT, when the packets corresponding to a single image successfully arrive at the sink node. For facilitating this DT synchronization, additional information is embedded in the transmitted image packets as application layer headers.

Fig. 7 illustrates the complete flow of the DT-based dynamic control process. The decision making component periodically acquires the BRISQUE score and the PDR value of the most recently received image at the sink from the DT. Concurrently, it continuously computes the running averages of the last three BRISQUE scores and the last three PDR values. The rationale behind using running averages is to enhance the reliability of the process. These running averages are then used as inputs for the fuzzy logic phase. The fuzzy logic phase comprises three fundamental sequential components : fuzzification, inference engine, and defuzzification. Firstly, during fuzzification, the crisp-valued inputs of BRISQUE score and PDR are transformed into fuzzy values using input membership functions. Next, using the fuzzy rule base, the inference engine applies IF-THEN rules to the inputs, resulting in the computation of the fuzzy output. Finally, in defuzzification, the fuzzy output is converted back to crisp values through the use of output membership functions.

Fig. 8 presents the membership functions for the three involved variables. The associated fuzzy rule base is provided in Table 2. DT What-if scenarios are employed to establish the membership functions and control rules, conducting a series of experiments using diverse configurations. Six rules are derived to guide the modification of the QC value at the source nodes. In general, if the BRISQUE score is within the *too good* range, then the QC value should *decrease* to conserve energy at the source node. In case, the BRISQUE score is *ideal*, then *no change* is required. The PDR comes in the equation only when the BRISQUE score is *bad*. If the BRISQUE score is *bad* while the PDR is *high*, this means that there are no issues with the network and the QC value should *increase* to improve the image quality. On the other hand, if the BRISQUE score is *bad* when the PDR is *low*, it indicates network congestion that could be mitigated by lowering the transmission datarate at the source node. For lowering the datarate, as discussed before, the QC value should *decrease*. After calculating the output, which represents the change in QC, it is then communicated to the respective source node. The source node receives the sent value and adds it to its current QC value. It is to be noted that the decision-making component only communicates with the source node if the output indicates a non-zero change in the value of QC. Furthermore, once feedback is provided to a source node, a waiting period of three subsequent image receptions is observed before the next feedback is sent. DT what-if scenarios were employed once more to identify a suitable waiting period. This approach struck a judicious balance, preventing overly abrupt reactions while ensuring the required responsiveness. A very short period would have been insufficient to comprehensively assess the actual traffic conditions in the network. This strategy yielded a favorable trade-off, enabling us to attain a high level of responsiveness alongside stability.

Table 2
Fuzzy rule base.

Rule #	BRISQUE	PDR	QC update
1	Too Good	High	Decrease
2	Too Good	Low	Decrease
3	Ideal	High	No Change
4	Ideal	Low	No Change
5	Bad	High	Increase
6	Bad	Low	Decrease

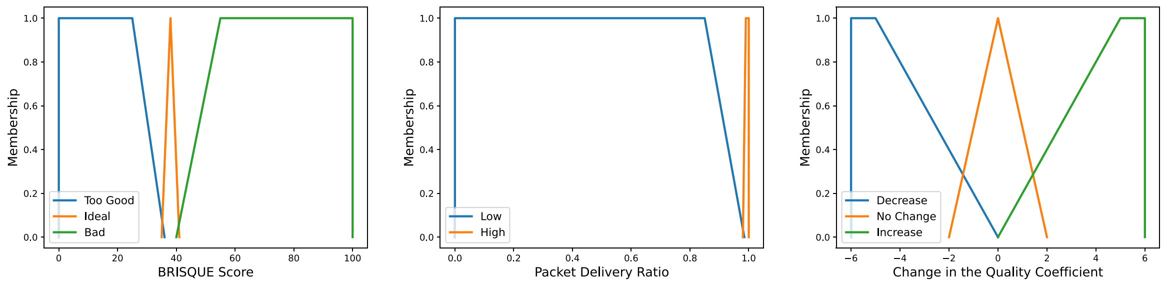

(a) Input variable - BRISQUE score (b) Input variable - PDR (c) Output variable - Change in QC

Fig. 8. Fuzzy membership functions for the input and the output variables.

5. Experimental setup and test scenarios

The implementation of the DT-informed real-time dynamic feedback or control stands as a fundamental characteristic of any DT system. The specifics of this dynamic control procedure depends upon the selected use-case. In order to validate the proposed system, we conduct experiments considering a real-world wetland scenario. Furthermore, we compare the performance of our system with that of a conventional WMSN-based monitoring system to demonstrate the effectiveness and utility of our approach. Our testing framework leverages open-source tools to demonstrate and exemplify the implementation of a simulated WMSN. This simulated approach is a prudent first step for verifying the system's functionalities during the initial design phase before deploying the actual WMSN testbed. Furthermore, we showcase the seamless integration of DT technology into the functioning of the WMSN. The fuzzy logic control is implemented through the utilization of a Python package called SciKit-Fuzzy [71].

Contiki-NG (Next Generation) [72] is a cross-platform operating system specifically developed for IoT devices operating in constrained environments. It concentrates on reliable low-power communications through the use of standardized protocols such as 6LoWPAN, IPv6, 6TiSCH, RPL, and CoAP. Therefore, it is an ideal choice for this work involving a WMSN. The Contiki-NG distribution also includes Cooja simulator that provides a simulated environment for running IEEE 802.15.4 networks. In the context of this work, Cooja simulator is utilized to simulate the WMSN for waterbirds monitoring, eliminating the need for Contiki-NG supported hardware. Furthermore, Contiki-NG facilitates a smooth and efficient transition from simulations to real hardware implementations. This way, virtually tested solutions are able to be seamlessly transferred and deployed on actual IoT devices.

The Cloud2Edge Package [73] from the Eclipse Foundation, utilized in this work, provides an integrated platform for DT development. It combines two different tools, namely, Hono [74] and Ditto [75]. Hono provides simplified connectivity to various types of IoT devices through several APIs that support protocols such as MQTT, CoAP, and HTTP [76]. Upon receiving telemetry data, Hono performs authentication before forwarding that data to Ditto. On the other hand, Ditto is solely for the purpose of creating and managing DTs in a standardized way. It employs a structured approach for organizing twin data into *things* comprising attributes and features that reflect the current state of the associated system. It provides several APIs that allow storage, update, and access to the latest twin data. The data hosted in Ditto could also be accessed by external applications and services. Figs. 9(a) and 9(b) displays the application twin and the network twin, respectively, as accessed from Ditto. The features other than the BRISQUE score and the PDR, contribute towards the usability of the DT.

In order to emulate the capture, encoding and transmission of real images, we made use of SenseVid [68]. SenseVid is a WSN specific image/video transmission and evaluation tool that employs the video traffic trace approach, enabling its usage in both simulation as well as real testbed networks. It performs images encoding and generates two trace files as output, namely the frame trace file, *st-frame*, contains information about the encoded image and the sender trace file, *st-packet*, informs about the data packets that are to be transmitted. On the receiving side, a trace file called *rt-packet* is used by SenseVid to rebuild the received image. Moreover, there is also an estimate about the energy spent on capturing and encoding each image.

Given that our proposal involves the incorporation of two additional features into a conventional WMSN-based monitoring setup, our approach entails selecting three test scenarios. We begin with a basic conventional WMSN, gradually introducing each feature one by one in the subsequent scenarios. By comparing the performance of each scenario to its preceding counterpart, we aim to clearly observe the benefits and improvements resulting from the addition of these features. The three considered scenarios are depicted in Fig. 10 and are described in the following subsections.

5.1. Scenario 1 — Conventional WMSN

The initial scenario comprises a straightforward simulated WMSN. The Cooja simulator is used to simulate the network nodes. In addition, to emulate the image capturing, encoding, transmission, reception, and decoding capabilities at the sources and the sink, Python scripts external of the Cooja simulator that incorporate SenseVid are utilized. The first Python script establishes a serial connection with a specific source node and sequentially forwards it the data packet sizes from all the *st-packet* trace files. These trace files are generated for all the images that are intended to be transmitted to the sink node. The source node continually listens on the connected serial socket. Upon receiving a serial message, it creates a data packet of a length corresponding to the size indicated in the message and forwards it towards the sink node. The intermediate nodes in the network simply forward the incoming packets to the next node. The first python script also takes care of the *(almost)* real-time transmission of the images. In order to clarify this, lets say there are 30 images to be captured, compressed, encoded, packetized, and transmitted to the sink node within 30 minutes. In this case, the interval between each image is 1 minute which means that all the packets in an *st-packet* file for a specific image should be transmitted to the sink node within this time period. This strict time constraint determines the inter-packet delay, which is quite crucial, as will be further discussed in the upcoming sections. The sink node receives the incoming packets from the source node and forwards it to the second Python script that is connected to it through a serial link. The second python script constructs the *rt-packet* trace file for all the received packets of an image in real-time and emulates image decoding using SenseVid.

In this scenario, which represents the operation of a basic WMSN, the source nodes continuously capture and transmit images to the sink node at regular intervals. However, in our waterbirds monitoring application, this continuous image transmissions can result in wastage of energy. It is possible that the camera triggers and sends images even when no waterbird is present, leading to increased energy consumption without meaningful data.

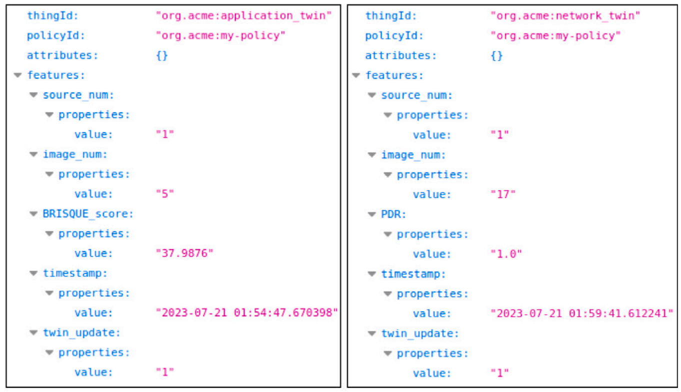

(a) Application Twin (b) Network Twin

Fig. 9. Digital Twin in Ditto.

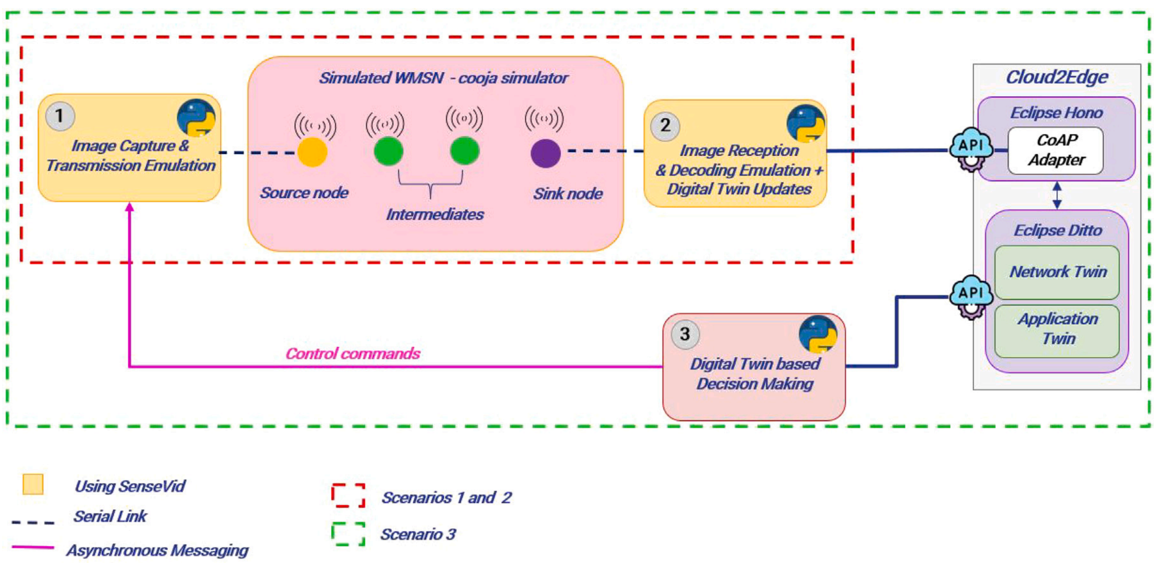

Fig. 10. Test setup for the three scenarios.

5.2. Scenario 2 — Energy-efficient WMSN

The second test scenario enhances the energy efficiency of the initial basic WMSN setup by incorporating a preliminary local audio identification stage at the source nodes. This enables the source nodes to identify the presence of waterbirds in the vicinity and selectively capture and transmit images only when absolutely necessary. However, the first Python script now takes into consideration the output of the preliminary local audio identification phase at the source nodes. Instead of continuously capturing and transmitting images in all the intervals, it selectively activates these processes only during intervals when the output indicates the presence of a waterbird. It is important to note that in this work, we do not focus on establishing the efficiency and accuracy of the techniques involved in the local audio identification, as they have already been addressed in our previous work [63,64]. Instead, our aim is to utilize the output of the identification stage as opposed to regular continuous transmissions, in order to observe the impact of such a strategy on the operation of the WMSN.

5.3. Scenario 3 — Energy-efficient DT-based WMSN

The third and final test scenario involves the integration of DT with the energy-efficient WMSN from the second test scenario. As shown in Fig. 10, this setup extends the scenario 2 by incorporating the DT-related tools alongside the existing components. Based on the considered research use-case, the second Python script updates the appropriate DT present inside the Cloud2Edge package. For updating the DT, the script sends commands to the Constrained Application Protocol (CoAP) adapter of Hono. CoAP is specialized for constrained devices and facilitates their connectivity to the wider Internet. Hono forwards the updates to Ditto where the DT are hosted. Inside Ditto, there are two DTs, one dedicated to the application and the other specific to the network. Ditto provides HTTP APIs to expose DTs to external applications. This enables the utilization of twin data for continuous intelligence, automated decision making and predictive maintenance by the incorporation of rules based on specific goals, optimization algorithms and advanced analytics. The third Python script is for the real-time decision making based on up-to-date information from the DT via the HTTP APIs. During the runtime of the application, this script utilizes the continuously updating information from the DT to asses the current state of the system and determine, based on the programmed logic, if a control command is required or not. In the current setup, the control is implemented through asynchronous messaging between the third and the first Python scripts (effectively at the source node). While the network could also be directly controlled, adjusting network parameters during runtime in Cooja simulator is quite challenging. Therefore, the approach of making changes at the source node is adopted.

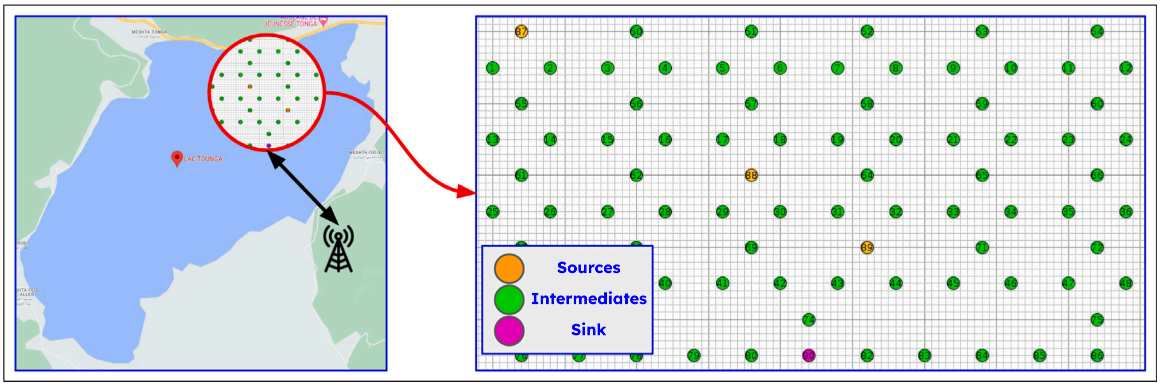

Fig. 11. The utilized network topology, inspired by a real wetland environment.

It should be noted that in a real system, the complete control path would involve communication from the DT to the sink node through the network to the source node. However, given the current emphasis on testing and validating the proposed system which contains some simulated and emulated components, direct asynchronous messaging between the relevant scripts proves to be sufficient. An essential clarification here is that the introduction of the DT may appear contradictory to the energy-efficiency goal pursued in the second test scenario, where we aim to increase the WMSN's lifespan. However, it is important to note that the local audio identification stage contributes in enhancing the energy efficiency of the source nodes which are assumed to be resource-constrained battery-powered devices. On the other hand, the DT is located at the sink side, where resources, including energy, are considered to be more abundant.

5.4. Network topology based on a real wetland

The WMSN topology utilized in Cooja for conducting the test scenarios is derived from our study on a prominent Algerian wetland known as Tonga Lake. Tonga Lake is situated in the National Park of El-Kala and is the most significant breeding area in North Africa for several different kinds of waterbirds. Fig. 11 presents our considered network topology consisting of three source nodes, several intermediates and a sink node. This topology is chosen in relation to the Tonga lake and its unique characteristics including the distribution of the waterbirds across the lake along with its dimensions. This information is determined through our visits to the site and consultation with forest conservation authorities. The nodes are intended to be placed across a 500 m × 960 m field. The three source nodes are assumed to be independent of each other, capturing audio and images that effectively lie outside each other's field of view. Each of the three source nodes has a varying number of hops distance to the sink node. The sink node is positioned at the center of the lower edge of the network. The transmission range of the nodes is around 80 meters. As stated before, the sink node is not resource-constrained like the other nodes in the network, which allows it to maintain a backhaul connection. Consequently, the DTs can be hosted remotely on the cloud, as the sink node can efficiently communicate with them.

Table 3 lists down the network settings of the Cooja simulator. In the simulated network, all nodes are of type Cooja and are configured to run the standard protocol stack. With this protocol stack, the physical layer of the network is based on the IEEE 802.15.4 standard, designed for devices having low-data-rate wireless connectivity with limited battery consumption requirements. The MAC layer uses Carrier-Sense Multiple Access (CSMA) while the network layer has Routing Protocol for Low-Power and Lossy Networks (RPL) [77]. The source nodes are programmed to run as a User Datagram Protocol (UDP) clients, while the sink node functions as a UDP server. The employed propagation model is the Unit Disk Graph Medium (UDGM).

Table 3
Network settings in Cooja.

Parameter	Value
Mote Type	Cooja Mote
Radio Medium	UDGM: Distance Loss
Transport Layer Protocol	UDP
Network Layer Protocol	RPL
MAC Layer Protocol	CSMA
Physical Layer	IEEE 802.15.4
Topology	Cluster
Number of Nodes	86

6. Results and discussion

In this section, we present and analyze the experimental results of our test scenarios. As previously discussed, we conduct a performance comparison for each scenario with its preceding counterpart to demonstrate the effectiveness of each newly added feature.

6.1. Test scenario 1 — Conventional WMSN

As mentioned earlier, in this test scenario, the source nodes continuously capture and transmit images to the sink node. In our experiments, all the source nodes operate simultaneously, with each node transmitting a set of 60 images. The time slot allocated for transmitting a single image is set at 40 s. Consequently, the total simulation time is approximately 40 minutes. More specifically, source node 1 transmits subsequent images from wetland scene 1 (Fig. 4(a)), source node 2 transmits subsequent images from wetland scene 2 (Fig. 4(b)), and source node 3 transmits subsequent images from wetland scene 3 (Fig. 4(c)). For all the three source nodes, the selected image resolution is 352 × 288 while the QC value is set at 20.

Fig. 12 displays the BRISQUE scores and the PDR values for the received images at the sink node. Notably, in this case, the per-image PDR remains consistently close to 1 throughout the simulation for all the images from the three sources, indicating good network conditions without any packet losses. Moreover, the BRISQUE scores for the received images from the source node 1 and the source node 2 exhibit considerable stability as evident from Figs. 12(a) and 12(c). On the other hand, the BRISQUE scores of the received images from the source node 2 show frequent fluctuations (Fig. 12(b)) with several high values, suggesting that the corresponding wetland scene may not be very visually clear.

In this test scenario, our primary focus is to observe the total energy consumption incurred by the application at the source nodes. The combined energy consumption of interest at the three source nodes can be calculated as follows :

$$E_{Total} = E_{source\_1} + E_{source\_2} + E_{source\_3} \tag{1}$$

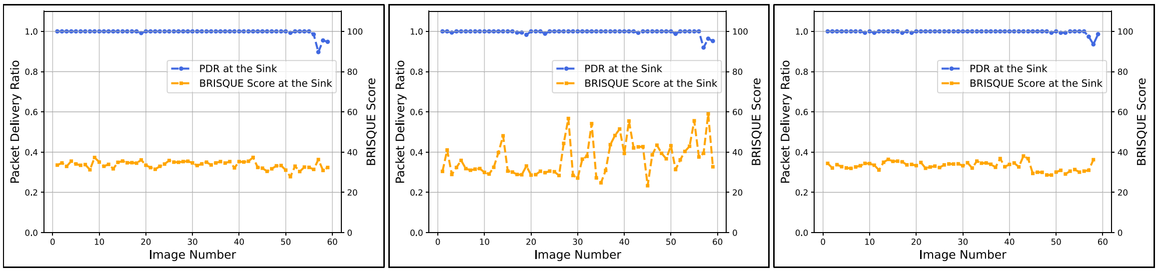

(a) Reception from the source node 1 (b) Reception from the source node 2 (c) Reception from the source node 3

Fig. 12. The BRISQUE scores and the PDR values at the sink node (Test scenario 1 — Conventional WMSN).

where E_{Total} is the total energy consumption while E_{source_1}, E_{source_2} and E_{source_3} denote the energy consumption of the source node 1, the source node 2 and the source node 3, respectively. At the individual source node level, the energy consumption attributable to our application is determined by the stages of image capturing, encoding, and transmission. Hence, the energy consumption at an individual source node can be given by :

$$E_{source} = N_{image}(E_{capture} + E_{encode} + E_{transmit}) \tag{2}$$

where E_{source} is the energy consumption of a specific source node and N_{image} is the number of transmitted images. Additionally, the energy consumption for capturing, encoding and transmitting a single image is given by $E_{capture}$, E_{encode} and $E_{transmit}$, respectively. The values of $E_{capture}$ and E_{encode} are computed by SenseVid, whereas we manually calculate $E_{transmit}$. The manual calculation of $E_{transmit}$ involves considering the number and size of the transmitted packets in each image along with making certain assumptions about the characteristics of the sensor nodes, such as data rate, and other relevant factors. These assumptions are previously well-defined in [64]. The combined energy consumption for this test scenario is calculated to be :

$$E_{Total} = E_{source\_1} + E_{source\_2} + E_{source\_3}$$

$$E_{Total} = 1.268 + 1.518 + 1.379$$

$$E_{Total} = 4.166 \text{ J}$$

6.1.1. Denoising and classification accuracy

Denoising, employed in scenarios 2 and 3, stands as a critical component of the audio identification process, as it effectively mitigates the detrimental impact of environmental disturbances prevalent in wetland areas. Without robust denoising, the audio identification task is susceptible to significant performance degradation. Therefore, our primary focus in this section lies in evaluating the influence of denoising on audio classification accuracy. To achieve this objective, we compiled a collection of 117 target calls from the *Xeno-canto database*.[1] Subsequently, these calls underwent contamination by diverse forms of natural noises, encompassing elements such as wind, rain, and other ambient sounds typical of lakeside environments. These contaminations were introduced at varying Signal To Noise Ratios (SNR) of 0 dB, 5 dB, and 10 dB. The selection of these specific SNR values resulted from a comprehensive set of listening tests designed to closely mimic real-world conditions.

Moreover, we included 50 additional recordings for evaluating the system's response to non-target sounds. Within this set, 30 recordings originated from 11 non-target bird species inhabiting the same ecosystem as the three target species. The remaining 20 recordings featured a diverse range of sounds, encompassing insects, water-related noises, and other fauna commonly encountered in proximity to lakes.

[1] https://xeno-canto.org/

Table 4
Confusion matrix.

Case	TP	FP	FN	TN
Without denoising	13	2	104	48
With denoising	93	2	24	48

To further serve as a reference, we incorporated 40 clean target audio samples, culminating in a total of 167 recordings subjected to testing. The performance of the classification process was assessed using a variety of metrics. To ascertain the effectiveness of our proposed audio identification approach, we considered the following metrics :

$$Precision = TP/(TP + FP)$$

$$Recall = TP/(TP + FN)$$

$$F\text{-}measure = 2 \ . \ Precision \ . \ Recall/(Precision + Recall)$$

$$Accuracy = (TP + TN)/(TP + TN + FP + FN)$$

where, TP, TN, FP, and FN represent the counts of true positives, true negatives, false positives, and false negatives, respectively. Precision measures the fraction of relevant audio data among the retrieved sounds in the dataset, while Recall (also known as Sensitivity) represents the ratio of correctly identified birds to the total number of relevant calls in the dataset. The F-measure is a metric that balances Precision and Sensitivity. Lastly, Accuracy indicates the proportion of correct predictions in the dataset. The corresponding confusion matrix can be found in Table 4.

Fig. 13 presents a visual comparison of the audio identification system's performance with and without denoising. Across all evaluated metrics, the results unequivocally demonstrate the significant performance gains achieved by employing denoising. The subpar performance observed in metrics such as *Recall*, *Accuracy*, and *F-measure* when denoising is not implemented can be attributed to the detrimental effects of environmental noise on audio calls. These distortions significantly hinder the system's ability to accurately identify the majority of target bird calls. In contrast, the system exhibits commendable performance in identifying non-target calls without denoising, primarily due to the stringent classification threshold employed, resulting in a notably high *Precision* value. This proficiency in recognizing non-target calls remains consistent when denoising is applied. However, denoising plays a crucial role in enhancing the precise identification of bird calls, ultimately leading to an overall superior performance across all metrics. Consequently, the denoising stage emerges as a pivotal component in the enhanced efficacy of the audio chain system.

6.2. Test scenario 2 — Energy-efficient WMSN

In this test scenario, a preliminary local audio identification stage is incorporated at the source nodes. Other than this, all other settings remain unchanged compared to the previous scenario. At the start of each time slot allocated for image transmission, it is assumed, that a 2-second long audio identification step is performed. In our simulations,

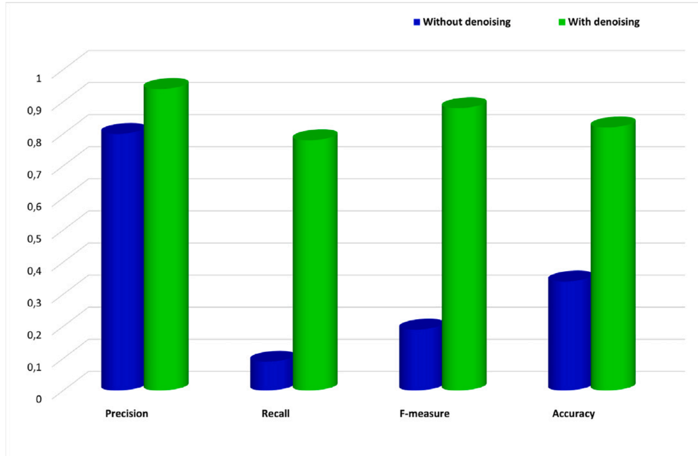

Fig. 13. Performance evaluation of the audio identification.

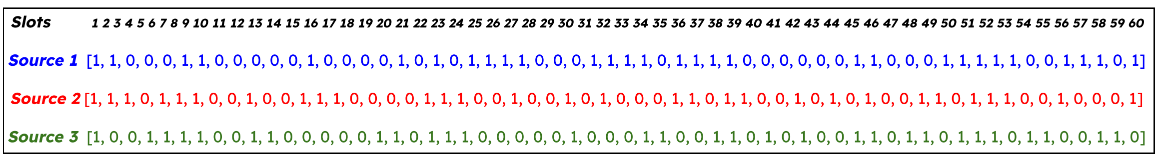

(a) Output sequences of the audio identification stage for all the three source nodes

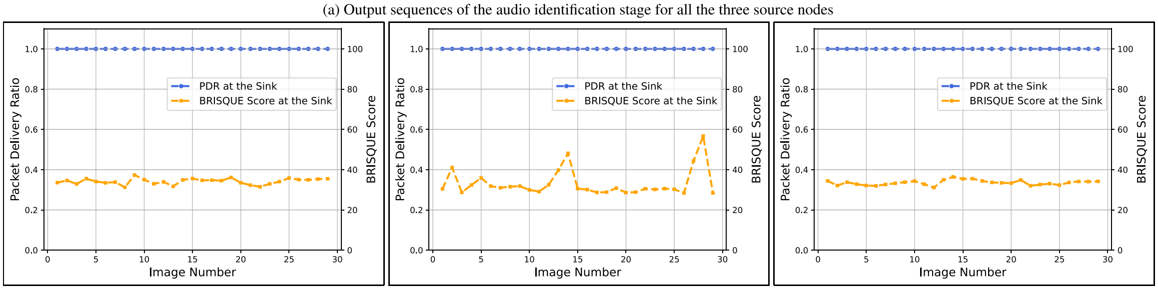

(b) Reception from the source node 1   (c) Reception from the source node 2   (d) Reception from the source node 3

Fig. 14. Output sequences along with the BRISQUE scores and the PDR values at the sink node for $\varrho = 0.5$ (Test scenario 2 — Energy-Efficient WMSN).

we directly utilize the output of this step to determine whether an image should be transmitted or not during a specific time slot. As previously discussed, we make statistical use of the output from the audio identification stage. Unlike the scenario 1, where continuous transmissions occurred in all the time slots, here we selectively transmit only in a percentage of those slots. This percentage corresponds to the probability (ϱ) that a waterbird occurs in one period. In our simulation, we utilize an output sequence that serves as a probabilistic representation of waterbird occurrences. The sequence consists of ones and zeroes and has a length equal to 60 which is the total number of time slots. Wherever there is a one in the sequence, it indicates the presence of a waterbird, and an image transmission occurs during that specific time slot. We generate this sequence using a specific value of ϱ. In Fig. 14, the results of the test scenario 2 for $\varrho = 0.5$ are presented. The utilized output sequences for the three sources are shown in Fig. 14(a), while the BRISQUE scores and the PDR values for the received images from the three sources at the sink node are displayed in Fig. 14(b), Fig. 14(c), and Fig. 14(d). It is to be noted that in this case, the image transmissions occur only in 50% of the total time slots. Furthermore, there is a strong likelihood that concurrent transmissions in the same slot by the three source nodes do not occur, leading to improved network conditions. The reduction in simultaneous transmissions reduces the risk of congestion and enhances the data transmission efficiency of the WMSN.

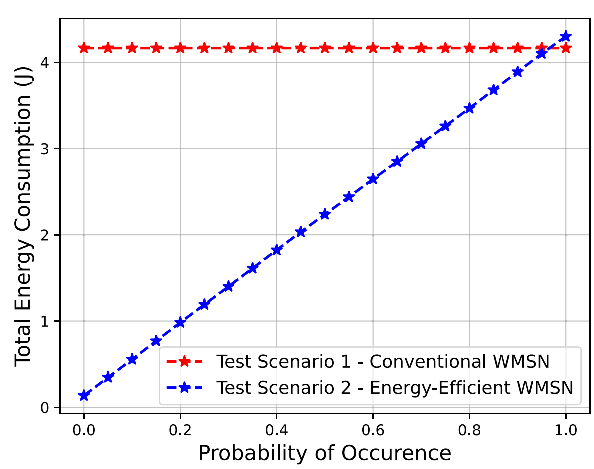

Fig. 15. E_{Total} vs ϱ for the test scenario 1 and 2.

In this scenario, we also take into consideration the energy consumption to facilitate a meaningful comparison with test scenario 1. Due to the addition of the local audio identification step, the energy

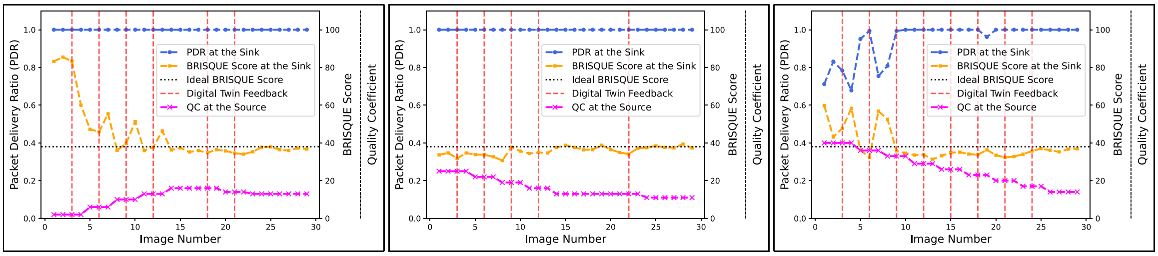

(a) Low starting QC value with perfect network conditions (b) High starting QC value with perfect network conditions (c) High starting QC value with network congestion

Fig. 16. The BRISQUE scores and the PDR values at the sink node for reception from the source node 1 at $\varrho = 0.5$ - (Test scenario 3 — Energy-Efficient DT-based WMSN).

consumption at an individual source node now becomes :

$$E_{source} = N_{image}(E_{capture} + E_{encode} + E_{transmit}) + N_{audio}E_{audio} \quad (3)$$

where N_{audio} is the number of time slots where the audio identification is employed while E_{audio} is the energy consumption of a single 2-second long audio identification step. The rest of the variables are the same as in Eq. (2). Given that the audio identification is utilized in all the 60 slots, $N_{audio} = 60$. Moreover, with a single 2-second long audio identification step, the energy consumption is calculated to be 0.00225 Joule [64] which makes $E_{audio} = 0.00225$ Joule. Fig. 15 presents a comparison of the test scenarios 1 and 2 with respect to the total combined energy consumption for all the three source nodes at different ϱ values. The graph clearly illustrates that the inclusion of the local audio identification stage results in a significant improvement in the total energy consumption. Particularly, at lower values of ϱ that represent more realistic cases, the test scenario 2 consumes significantly less energy as compared to the scenario 1. The scenario 1, irrespective of the ϱ value, consumes constant energy of 4.166 Joule throughout. However, only when ϱ exceeds 0.95 (rare in real wetland environments), test scenario 1 become more energy-efficient, but only marginally so.

6.3. Test scenario 3 — Energy-efficient DT-based WMSN

This test scenario builds upon the previous one by adding DT into the operation of the energy-efficient WMSN. We demonstrate the effectiveness of utilizing DT in the specific use-case involving dynamic control of the QC values at the source nodes, as already explained in Section 4.4. We conduct our experiments using the same settings as in the previous scenarios. The sole variation lies in setting different initial QC values at the source nodes to achieve distinct conditions, showcasing how the DT dynamically help the system to attain optimal performance across diverse circumstances. Fig. 16 presents the results from the test scenario 3 with $\varrho = 0.5$. It should be noted that while the DT-based dynamic control is simultaneously applied to all the three source nodes, for the sake of discussion, we primarily focus on the source node 1. Figs. 16(a) and 16(b) demonstrate the cases where network conditions are perfect, with no packet losses. However, the initial QC value is not set near the ideal value, resulting in either low-quality received images at the sink node or unnecessary energy wastage at the source node. From Fig. 16(a), it can be observed that the initial QC value is set at 2, which is too low, resulting in excessively high BRISQUE scores for the received images at the sink. Through the DT-based dynamic control utilizing fuzzy logic, continuous analysis takes place, leading to regular feedback being sent to the source node to change the current QC value. As a result, within a few transmissions, the QC value is adjusted, and the received images begin to demonstrate quality closer to the ideal BRISQUE score. Similarly, in Fig. 16(b), the initial QC value is set at 25, which is too high. Consequently, the received images are of overly high quality, leading to energy wastage at the source node. However, through the DT-based dynamic control mechanism, the QC value is adjusted to bring the quality of received images closer to the ideal BRISQUE score, sufficient for the application's requirements. Lastly, in Fig. 16(c), network congestion can be seen which is created by setting excessively high QC values at all the three source nodes. This congestion leads to a drop in the PDR values for the first few received images at the sink node. As evident, the lowered PDR values correspond to an increase in the BRISQUE scores since the visual quality of the received images deteriorates due to the packet losses. But here again the DT-based dynamic control and optimization come into play, efficiently adapting the QC values at the source nodes. This adaptive control process rectifies the situation, improving the network condition and bringing the BRISQUE scores closer to the ideal value.

6.4. Impact of increasing the number of sources

In this subsection, we investigate the impact of increasing the number of sources simultaneously transmitting images on the three scenarios. Fig. 17 illustrates the consequences of escalating the number of sources, ranging from a single-node source to six sources, on both QoS and QoE metrics. Our findings reveal that increased source density can negatively impact network performance in terms of both QoS and QoE metrics across all three scenarios.

Fig. 17(a) depicts the relationship between the average PDR scores and the number of sources. As expected, the PDR decreases with the increase in source density, primarily due to network congestion caused by heavy traffic. Notably, Scenario 1 exhibits significantly lower PDR averages compared to Scenarios 2 and 3, primarily attributed to the absence of adaptive image selection. This results in the transmission of unnecessary images, further exacerbating network congestion. We observe that Scenario 3 consistently outperforms Scenario 2 in terms of PDR due to its adopted dynamic network traffic control.

Based on our qualitative assessment of image quality, we established a minimum acceptable benchmark for PDR at 0.80. This criterion effectively indicates the threshold beyond which image quality degradation becomes noticeable. Accordingly, the capacity to support simultaneous transmissions from multiple sources varies across the three scenarios. Scenario 1 can accommodate a maximum of three sources transmitting concurrently while still maintaining an acceptable PDR. Scenario 2 extends this capacity to four sources, while Scenario 3 allows for the inclusion of up to five sources, all while meeting the minimum allowed PDR.

Fig. 17(b) presents the average scores of the BRISUQE metric in relation to the number of sources. Scenario 1 exhibits the most pronounced increase in BRISUQE values as the number of sources increases, indicating a more significant degradation in image quality compared to Scenarios 2 and 3. This trend highlights the limitations of Scenario 1 in handling increasing traffic demands while maintaining acceptable image quality. For the scalability study, the threshold for acceptable BRISUQE scores is set to 50. In Scenario 1, a maximum of four sources can be accommodated while maintaining acceptable image quality. Similarly, Scenario 2 can support up to four sources, and Scenario 3

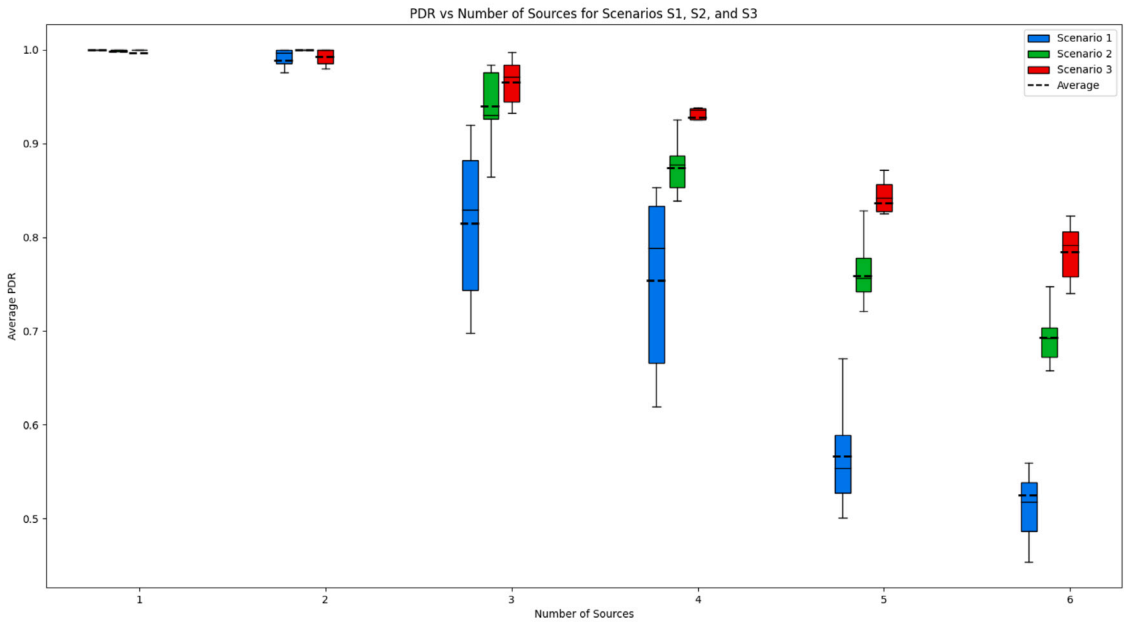

(a) PDR average

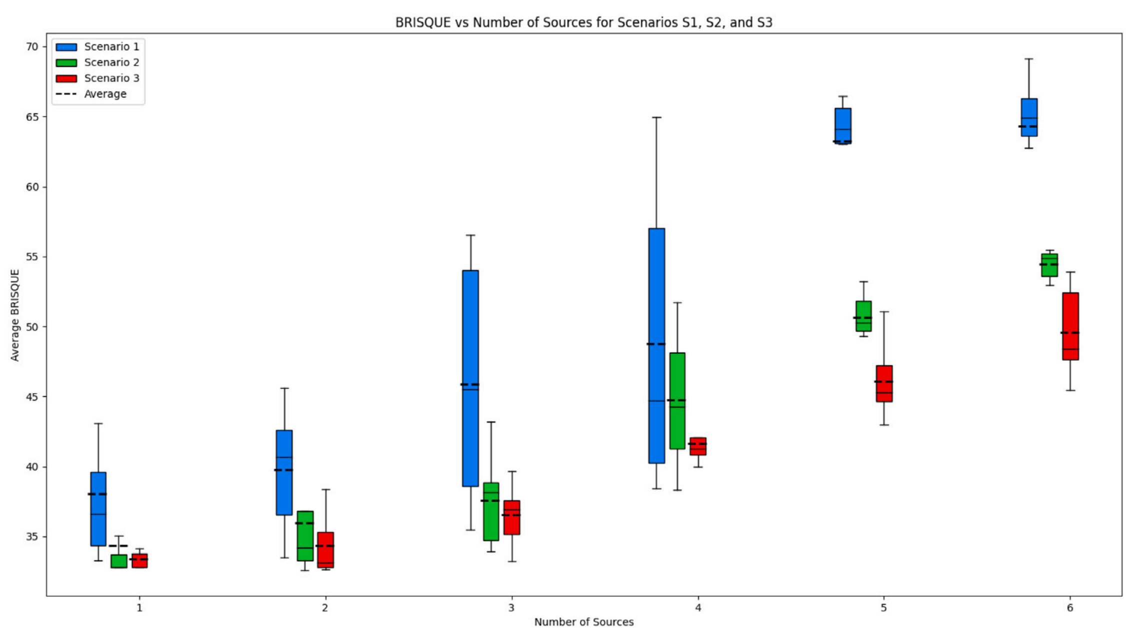

(b) BRISUQE average

Fig. 17. Multi-Source Impact on QoE and QoS.

allows for the inclusion of up to six sources, all while ensuring the preservation of acceptable image quality.

While the proposed system demonstrates superior performance in maintaining image quality, our analysis reveals that increasing the number of sources transmitting images simultaneously can have detrimental effects on network performance, leading to decreased PDR, increased image quality degradation, and potential synchronization issues with the Digital Twin. To address this scalability challenge, we anticipate leveraging the DT's global perspective to enable intelligent scheduling of the sources. Transmissions can be scheduled proactively to prevent a complete network blackout and maintain the overall integrity of the monitoring system.

Last but not least, we intend to move from the simulated space to physical implementation in a real wetland. This would warrant appropriate modifications, particularly in terms of implementing the DT feedback path through the network.

7. Conclusion

This work envisions a DT-based energy-efficient WMSN for waterbirds monitoring that leverages two synergistic enhancements to a conventional WMSN setup. Firstly, a real-time local low-complexity audio identification phase is integrated to decide when to activate the camera for image capture, thus conserving energy at the source nodes. Additionally, a DT is introduced to function as a software replica of the system We demonstrate its effectiveness in a real-world wetland setting through experiments encompassing three scenarios. A basic WMSN forms the baseline, followed by an energy-efficient WMSN and an energy-efficient DT-based WMSN. Our experiments employing a dynamic control use-case involving real-time adaptation of image compression rate at the source nodes demonstrate the proposed system's superior energy efficiency compared to conventional WMSNs and its dynamic adaptability to maintain required performance, attributed to the DT integration.

The employment of fuzzy logic in our setup serves as a proof-of-concept for showcasing DT's utility in system analysis and decision-making with dynamic feedback control. Alternative approaches, such as AI-based optimization algorithms, warrant exploration for enhanced decision-making strategies. We plan to explore a few different algorithms for the DT-based decision making process, aiming to identify the most effective among them. For instance, a holistic decision-making approach encompassing all data flows could be investigated.

The "what-if scenarios" feature of the implemented DTs has been effectively leveraged to rapidly obtain initial yet effective parameter settings for the decision-making algorithm. As a future work, we expect to dynamically adjust the different parameters involved (waiting period, fuzzy membership functions and rules, …) to closely mirror the network dynamics.

While the proposed system demonstrates superior performance in maintaining image quality, our analysis reveals that increasing the number of sources transmitting images simultaneously can have detrimental effects on network performance, leading to decreased PDR, increased image quality degradation, and potential synchronization issues with the Digital Twin. To address this scalability challenge, we anticipate leveraging the DT's global perspective to enable intelligent scheduling of the sources. Transmissions can be optimally scheduled to prevent a complete network blackout and maintain the overall integrity of the monitoring system.

Last but not least, we intend to move from the simulated space to physical implementation in a real wetland. This would warrant appropriate modifications particularly in terms of implementing the DT feedback path through the network.

CRediT authorship contribution statement

Aya Sakhri: Data curation, Writing – original draft, Writing – review & editing. **Arsalan Ahmed:** Software, Writing – original draft. **Moufida Maimour:** Conceptualization, Funding acquisition, Investigation, Methodology, Project administration, Software, Supervision, Validation, Writing – original draft, Writing – review & editing. **Mehdi Kherbache:** Software, Writing – original draft. **Eric Rondeau:** Funding acquisition, Project administration, Supervision, Conceptualization, Validation. **Noureddine Doghmane:** Funding acquisition, Supervision, Validation.

Declaration of competing interest

The authors declare that they have no known competing financial interests or personal relationships that could have appeared to influence the work reported in this paper.

Data availability

Data will be made available on request.

Acknowledgments

This work is supported in part by the PHC TASSILI 21MDU323 and the Erasmus Mundus Joint Masters Degree program in GrEen NetworkIng And cLoud computing (GENIAL MSCA-EMJMD-2019).

References

[1] S. Hu, Z. Niu, Y. Chen, L. Li, H. Zhang, Global wetlands: Potential distribution, wetland loss, and status, Sci. Total Environ. 586 (2017) 319–327.
[2] R.C. Gardner, S. Barchiesi, C. Beltrame, C. Finlayson, T. Galewski, I. Harrison, M. Paganini, C. Perennou, D. Pritchard, A. Rosenqvist, et al., State of the world's wetlands and their services to people: A compilation of recent analyses.
[3] United Nations, Wetlands disappearing three times faster than forests, 2023, (Last Accessed: December 2023).
[4] J.A. Amat, A.J. Green, Waterbirds as bioindicators of environmental conditions, in: Conservation Monitoring in Freshwater Habitats, Springer, 2010, pp. 45–52.
[5] W. Wei Zhang, J. Zhang Ma, Waterbirds as bioindicators of wetland heavy metal pollution, Procedia Environ. Sci. 10 (2011) 2769–2774.
[6] Wetlands International, Waterbird population estimates: Fifth edition - summary, 2012, (Last Accessed : December 2023).
[7] I.F. Akyildiz, T. Melodia, K.R. Chowdhury, A survey on wireless multimedia sensor networks, Comput. Netw. 51 (4) (2007) 921–960.
[8] M. Ringwald, K. Romer, Deployment of sensor networks: Problems and passive inspection, in: 2007 Fifth Workshop on Intelligent Solutions in Embedded Systems, IEEE, 2007, pp. 179–192.
[9] B.R. Barricelli, E. Casiraghi, D. Fogli, A survey on digital twin: Definitions, characteristics, applications, and design implications, IEEE Access 7 (2019) 167653–167671.
[10] F. Tao, H. Zhang, A. Liu, A.Y. Nee, Digital twin in industry: State-of-the-art, IEEE Trans. Ind. Inf. 15 (4) (2018) 2405–2415.
[11] E. Glaessgen, D. Stargel, The digital twin paradigm for future nasa and us air force vehicles, in: 53rd AIAA/ASME/ASCE/AHS/ASC Structures, Structural Dynamics and Materials Conference 20th AIAA/ASME/AHS Adaptive Structures Conference 14th AIAA, 2012, p. 1818.
[12] M. Grieves, Digital twin: manufacturing excellence through virtual factory replication, White Paper 1 (2014) (2014) 1–7.
[13] G. Top, Strategic Technology Trends for 2019, vol. 10, (no. 10) David Cearley, Brian Burke.
[14] Centre for Digital Built Britain, What are connected digital twins?, Gemini Papers.
[15] A. Fuller, Z. Fan, C. Day, C. Barlow, Digital twin: Enabling technologies, challenges and open research, IEEE access 8 (2020) 108952–108971.
[16] L.A. Zadeh, Fuzzy sets, Inf. Control 8 (3) (1965) 338–353.
[17] F. Dernoncourt, Introduction to Fuzzy Logic, vol. 21, Massachusetts Institute of Technology, 2013, pp. 50–56.
[18] T. Sheltami, M. Musaddiq, E. Shakshuki, Data compression techniques in wireless sensor networks, Future Gener. Comput. Syst. 64 (2016) 151–162.
[19] W. Feng, C. Hu, Y. Wang, J. Zhang, H. Yan, A novel hierarchical coding progressive transmission method for WMSN wildlife images, Sensors 19 (4) (2019) 946.
[20] A. Aliouat, N. Kouadria, S. Harize, M. Maimour, An efficient low complexity region-of-interest detection for video coding in wireless visual surveillance, IEEE Access 11 (2023) 26793–26806.
[21] A. Aliouat, N. Kouadria, M. Maimour, S. Harize, N. Doghmane, Region-of-interest based video coding strategy for rate/energy-constrained smart surveillance systems using wmsns, Ad Hoc Netw. 140 (2023) 103076.
[22] O. Hadji, O. Kadri, M. Maimour, E. Rondeau, A. Benyahia, Region of interest and redundancy problem in migratory birds wild life surveillance, in: 2022 International Conference on Advanced Aspects of Software Engineering, ICAASE, 2022, pp. 1–8, http://dx.doi.org/10.1109/ICAASE56196.2022.9931576.
[23] Y.A.U. Rehman, M. Tariq, T. Sato, A novel energy efficient object detection and image transmission approach for wireless multimedia sensor networks, IEEE Sensors J. 16 (15) (2016) 5942–5949.
[24] H. Oztarak, T. Yilmaz, K. Akkaya, A. Yazici, Efficient and accurate object classification in wireless multimedia sensor networks, in: 2012 21st International Conference on Computer Communications and Networks, ICCCN, IEEE, 2012, pp. 1–7.
[25] A. Zam, M.R. Khayyambashi, A. Bohlooli, Energy-aware strategy for collaborative target-detection in wireless multimedia sensor network, Multimedia Tools Appl. 78 (13) (2019) 18921–18941.
[26] M.S. Alhilal, A. Soudani, A. Al-Dhelaan, Low power scheme for image based object identification in wireless multimedia sensor networks, in: 2014 International Conference on Multimedia Computing and Systems, ICMCS, IEEE, 2014, pp. 927–932.
[27] S.-H. Ou, C.-H. Lee, V.S. Somayazulu, Y.-K. Chen, S.-Y. Chien, On-line multi-view video summarization for wireless video sensor network, IEEE J. Sel. Top. Sign. Proces. 9 (1) (2014) 165–179.

[28] A. Aliouat, N. Kouadria, M. Maimour, S. Harize, EVBS-CAT: enhanced video background subtraction with a controlled adaptive threshold for constrained wireless video surveillance, J. Real-Time Image Process. 21 (9) (2024) http://dx.doi.org/10.1007/s11554-023-01388-3.

[29] A.N. Sukumaran, R. Sankararajan, M. Swaminathan, Compressed sensing based foreground detection vector for object detection in wireless visual sensor networks, AEU-Int. J. Electron. Commun. 72 (2017) 216–224.

[30] S.A. Nandhini, S. Radha, R. Kishore, Efficient compressed sensing based object detection system for video surveillance application in WMSN, Multimedia Tools Appl. 77 (2) (2018) 1905–1925.

[31] M. Chen, S. González, H. Cao, Y. Zhang, S.T. Vuong, Enabling low bit-rate and reliable video surveillance over practical wireless sensor network, J. Supercomput. 65 (1) (2013) 287–300.

[32] M. Magno, F. Tombari, D. Brunelli, L. Di Stefano, L. Benini, Multimodal video analysis on self-powered resource-limited wireless smart camera, IEEE J. Emerg. Sel. Top. Circuits Syst. 3 (2) (2013) 223–235.

[33] M. Koyuncu, A. Yazici, M. Civelek, A. Cosar, M. Sert, Visual and auditory data fusion for energy-efficient and improved object recognition in wireless multimedia sensor networks, IEEE Sens. J. 19 (5) (2018) 1839–1849.

[34] IBM, What is a digital twin?.

[35] M. Maimour, A. Ahmed, E. Rondeau, Survey on digital twins for natural environments : a communication network perspective, Elsevier Internet of Things (ISSN: 2542-6605) (2024) http://dx.doi.org/10.1016/j.iot.2024.101070.

[36] H. Zhang, R. Wang, C. Wang, Monitoring and warning for digital twin-driven mountain geological disaster, in: 2019 IEEE International Conference on Mechatronics and Automation, ICMA, 2019, pp. 502–507, http://dx.doi.org/10.1109/ICMA.2019.8816292.

[37] W. Li, C. Zhang, System architecture and core technology, method and data-driven technology of digital twin riverbasin, in: 2022 IEEE 13th International Conference on Software Engineering and Service Science, ICSESS, 2022, pp. 105–109, http://dx.doi.org/10.1109/ICSESS54813.2022.9930231.

[38] L. Buonocore, J. Yates, R. Valentini, A proposal for a forest digital twin framework and its perspectives, Forests 13 (4) (2022) 498, http://dx.doi.org/10.3390/f13040498.

[39] C. Chioni, C. Pezzica, S. Favargiotti, Territorial digital twins: A key for increasing the community resilience of fragile mountain inner territories? Sustain. Develop. (2023).

[40] T. Huang, C. David, C. Oadia, J.T. Roberts, S.V. Kumar, P. Stackhouse, D. Borges, S. Baillarin, G. Blanchet, P. Kettig, An earth system digital twin for flood prediction and analysis, in: IGARSS 2022-2022 IEEE International Geoscience and Remote Sensing Symposium, IEEE, 2022, pp. 4735–4738, http://dx.doi.org/10.1109/IGARSS46834.2022.9884830.

[41] W. Li, M. Yang, B. Xi, Q. Huang, Framework of virtual plantation forest modeling and data analysis for digital twin, Forests 14 (4) (2023).

[42] S. Aheleroff, R.Y. Zhong, X. Xu, Z. Feng, P. Goyal, Digital twin enabled mass personalization: A case study of a smart wetland maintenance system, in: Volume 2: Manufacturing Processes; Manufacturing Systems; Nano/Micro/Meso Manufacturing; Quality and Reliability of International Manufacturing Science and Engineering Conference, 2020, http://dx.doi.org/10.1115/MSEC2020-8363.

[43] T.R. Allen, S. Katragadda, Y.-H. Chen, B. Terry, J. Baptist, O. Yetkin, N. Tahvildari, S. Han, B. Steiner, G. McLeod, S. Dangendor, Q. Sun, H. Richter, A digital twin to link flood models, sensors, and earth observations for coastal resilience in Hampton roads, Virginia, U.S.A, in: IGARSS 2023-2023 IEEE International Geoscience and Remote Sensing Symposium, 2023, pp. 1388–1391, http://dx.doi.org/10.1109/IGARSS52108.2023.10283168.

[44] D. Park, H. You, A digital twin dam and watershed management platform, Water 15 (11) (2023) http://dx.doi.org/10.3390/w15112106.

[45] L. Fariza, K. Kairat, A. Karlygash, B. Saule, B. Alina, I. Rauza, Digital twin of the quality management system for environmental control of the near-airdom environment, J. Theoretical Appl. Inf. Technol. 101 (12).

[46] A. Barbie, N. Pech, W. Hasselbring, S. Flögel, F. Wenzhöfer, M. Walter, E. Shchekinova, M. Busse, M. Türk, M. Hofbauer, S. Sommer, Developing an underwater network of ocean observation systems with digital twin prototypes - A field report from the Baltic sea, IEEE Internet Comput. 26 (3) (2022) 33–42, http://dx.doi.org/10.1109/MIC.2021.3065245.

[47] A. Tarpanelli, B. Bonaccorsi, M. Sinagra, A. Domeneghetti, L. Brocca, S. Barbetta, Flooding in the digital twin earth: the case study of the Enza River Levee Breach in 2017, Water 15 (9) (2023) http://dx.doi.org/10.3390/w15091644.

[48] D. Zhao, X. Li, X. Wang, X. Shen, W. Gao, Applying digital twins to research the relationship between urban expansion and vegetation coverage: A case study of natural preserve, Front. Plant Sci. 13 (2022) 134, http://dx.doi.org/10.3389/fpls.2022.840471.

[49] P. Jiang, N. Meinert, H. Jordão, C. Weisser, S. Holgate, A. Lavin, B. Lütjens, D. Newman, H. Wainwright, C. Walker, et al., Digital Twin Earth–Coasts: Developing a fast and physics-informed surrogate model for coastal floods via neural operators, arXiv preprint arXiv:2110.07100.

[50] U.P.A. Pillai, N. Pinardi, J. Alessandri, I. Federico, S. Causio, S. Unguendoli, A. Valentini, J. Staneva, A digital twin modelling framework for the assessment of seagrass nature based solutions against storm surges, Sci. Total Environ. 847 (2022) 157603, http://dx.doi.org/10.1016/j.scitotenv.2022.157603.

[51] Z. Zlatev, I. Dimov, Using a digital twin to study the influence of climatic changes on high ozone levels in Bulgaria and Europe, Atmosphere 13 (6) (2022) 932.

[52] K. Hyeong-su, K. Jin-Woo, S. Yun, W.-T. Kim, A novel wildfire digital-twin framework using interactive wildfire spread simulator, in: 2019 Eleventh International Conference on Ubiquitous and Future Networks, ICUFN, IEEE, 2019, pp. 636–638.

[53] M. Mõttus, M. Dees, H. Astola, S. Dalek, E. Halme, T. Hame, M. Krzyzanowska, A. Makela, G. Marin, F. Minunno, et al., A methodology for implementing a digital twin of the earth's forests to match the requirements of different user groups, in: GI Forum 9 (2021) 130–136.

[54] Y. Liu, Z. Xiaofe, W. Huang, D. He, X. Mi, A framework for rare and endangered plants protection based on beidou and digital twins technology, in: 2021 International Conference on Electronic Information Technology and Smart Agriculture, ICEITSA, 2021, pp. 130–134, http://dx.doi.org/10.1109/ICEITSA54226.2021.00034.

[55] G. Sanchez-Guzman, W. Velasquez, M.S. Alvarez-Alvarado, Modeling a simulated forest to get burning times of tree species using a digital twin, in: 2022 IEEE 12th Annual Computing and Communication Workshop and Conference, CCWC, IEEE, 2022, pp. 0639–0643.

[56] A. Komninos, G. Tsigkas, Prototyping a digital twin system for environmental education, in: Proceedings of the 26th Pan-Hellenic Conference on Informatics, PCI'22, Association for Computing Machinery, 2022, pp. 361–366, http://dx.doi.org/10.1145/3575879.3576018.

[57] M. Kherbache, M. Maimour, E. Rondeau, Network digital twin for the industrial Internet of Things, in: 2022 IEEE 23rd International Symposium on a World of Wireless, Mobile and Multimedia Networks, WoWMoM, IEEE, 2022, pp. 573–578.

[58] C. Zhou, H. Yang, X. Duan, D. Lopez, A. Pastor, Q. Wu, M. Boucadair, C. Jacquenet, Digital twin network: concepts and reference architecture, internet-draft draft-irtf-nmrg-network-digital-twin-arch-04, Internet Engineering Task Force, work in Progress (Oct. 2023).

[59] P. Almasan, M. Ferriol-Galmés, J. Paillisse, J. Suárez-Varela, D. Perino, D. López, A. Perales, et al., Network digital twin: Context, enabling technologies, and opportunities, IEEE Commun. Mag. 60 (11) (2022) 22–27, http://dx.doi.org/10.1109/MCOM.001.2200012.

[60] L.U. Khan, Z. Han, W. Saad, E. Hossain, M. Guizani, C.S. Hong, Digital twin of wireless systems: Overview, taxonomy, challenges, and opportunities, arXiv preprint arXiv:2202.02559.

[61] Y. Zhu, D. Chen, C. Zhou, L. Lu, X. Duan, A knowledge graph based construction method for digital twin network, in: 2021 IEEE 1st International Conference on Digital Twins and Parallel Intelligence, DTPI, 2021, pp. 362–365, http://dx.doi.org/10.1109/DTPI52967.2021.9540177.

[62] M. Ferriol-Galmés, J. Suárez-Varela, J. Paillise, X. Shi, S. Xiao, X. Cheng, P. Barlet-Ros, A. Cabellos-Aparicio, Building a digital twin for network optimization using graph neural networks, Available at SSRN 3995236.

[63] A. Sakhri, O. Hadji, C. Bouarrouguen, M. Maimour, N. Kouadria, A. Benyahia, E. Rondeau, N. Doghmane, S. Harize, Audio-visual low power system for endangered waterbirds monitoring, IFAC-PapersOnLine 55 (5) (2022) 25–30.

[64] A. Sakhri, M. Maimour, E. Rondeau, N. Doghmane, S. Harize, An energy-efficient WMSN-based system for endangered birds monitoring, IFAC-PapersOnLine 55 (8) (2022) 77–82.

[65] Y. Lu, P.C. Loizou, A geometric approach to spectral subtraction, Speech Commun. 50 (6) (2008) 453–466.

[66] Feature extraction using MFCC, Shikha Gupta, Jafreezal Jaafar, W.F. Wan Ahmad, Arpit Bansal, Signal Image Process.: Int. J. 4 (4) (2013) 101–108.

[67] M. Müller, Dynamic time warping, in: Information retrieval for music and motion, 2007, pp. 69–84.

[68] M. Maimour, SenseVid: A traffic trace based tool for QoE video transmission assessment dedicated to wireless video sensor networks, Simul. Model. Pract. Theory 87 (2018) 120–137.

[69] A. Mittal, A.K. Moorthy, A.C. Bovik, No-reference image quality assessment in the spatial domain, IEEE Trans. Image Process. 21 (12) (2012) 4695–4708.

[70] Z. Wang, A. Bovik, H. Sheikh, E. Simoncelli, Image quality assessment: From error visibility to structural similarity, IEEE Trans. Image Process. 13 (4) (2004) 600–612.

[71] J. Warner, 2019. SciKit-Fuzzy. [Last Accessed December 2023].

[72] G. Oikonomou, S. Duquennoy, A. Elsts, J. Eriksson, Y. Tanaka, N. Tsiftes, The contiki-NG open source operating system for next generation IoT devices, SoftwareX 18 (2022) 101089.

[73] Eclipse, 2023. Cloud2Edge. (Last Accessed December 2023).

[74] Eclipse, Connect, command & control IoT devices, 2023, (Last Accessed December 2023).

[75] Eclipse, Eclipse Ditto™ • open source framework for digital twins in the IoT, 2023, (Last Accessed December 2023).

[76] M. Kherbache, M. Maimour, E. Rondeau, Digital twin network for the IIoT using eclipse Ditto and Hono, IFAC-PapersOnLine 55 (8) (2022) 37–42.

[77] R. Alexander, A. Brandt, J. Vasseur, J. Hui, K. Pister, P. Thubert, P. Levis, R. Struik, R. Kelsey, T. Winter, RPL: IPv6 routing protocol for low-power and lossy networks, 2012, http://dx.doi.org/10.17487/RFC6550, RFC 6550.

Aya Sakhri received the M.Sc. degree in Networks and Telecommunications in 2021. She is currently a Ph.D. student at University of Lorraine, France and Badji Mokhtar University, Algeria. Her current research interests include waterbirds monitoring, wireless multimedia sensor networks and deep learning.

Arsalan Ahmed received the B.Sc. degree in Electrical Engineering with a minor in Computer Science from Habib University, Pakistan in 2021. He is currently a graduate student as part of the Erasmus Mundus Joint Masters Degree in GENIAL (GrEen NetworkIng And cLoud computing). His current research interests include digital twins, wireless sensor networks and sustainable communication networks.

Moufida Maimour has been an Associate Professor at Lorraine University, Nancy, France, since 2004, and is a member of the Centre de Recherches en Automatique de Nancy (CRAN). She earned her engineering degree in computer science from the University of Constantine, Algeria, in 1998, and completed her Ph.D. at Claude Bernard University in 2003. Her doctoral research was conducted at the Laboratoire Informatique du Parralélisme (LIP), ENS Lyon, France. During this period, her primary focus was on reliable multicast and congestion control on the internet, and she actively contributed to numerous networking and grid computing projects. Presently, her research pursuits encompass wireless sensor networks, knowledge-defined networks, and digital twinning for the IoT, with a specific emphasis on the Industrial Internet of Things (IIoT) and the Internet of Multimedia Things (IoMT).

Mehdi Kherbache got his engineering degree from the Higher National School of Computer Science, Algiers in 2020. He is currently pursuing a Ph.D at the Research Center of Automatic Control, Lorraine University since 2020. His research interests mainly focus on Industrial Internet of Things, Network Digital Twins and TSCH scheduling using reinforcement learning.

Eric Rondeau (60) is professor at University of Lorraine since 2012. His expertise covers network engineering and more specifically real-time communications and green networking. He supervised 18 PHD theses. He published more than 180 papers in journals, conferences and book chapters. He has a strong experience in European projects. From 2004, He was the general coordinator of FP6-STREP European project on Neworked Control Systems Tolerant to faults (NeCST) for 4 years. He was the director of Erasmus Mundus Master (EMM) in PERCCOM: PERvasive Computing and COMmunications for sustainable development (2012-2019). He is currently involved in RedWolf Interreg Project (Rethink Electricity Distribution Without Load Following) and he is local coordinator of EMM in GENIAL (GrEen NetworkIng And cLoud computing). He was the member of IFAC TC 1.5 on Networked Systems and is now the vice president of IFAC TC 8.3 on Modelling and Control of Environment System.

Noureddine Doghmane Received his engineering degree in electronics from Annaba University, Algeria, in 1984 and his PhD from Lyon University Claude Bernard, France, in 1988. He is now a professor in the University of Annaba, Algeria. He is also member of the laboratory of automatic and signal processing of Annaba (LASA). His main research interests include signal processing, digital communications and image/video coding.